

The Influence of Climate Change and Variability on Spatio-Temporal Rainfall and Temperature Distribution in Zanzibar

Abdalla Hassan Abdalla¹, Kombo Hamad Kai¹, Sara Abdalla Khamis²,
Afredy Lawrence Kondowe², Sarah E. Osima², Philemon Henry King'uzza², Asya Omar Hamad²

¹Tanzania Meteorological Authority (TMA), Zanzibar, Tanzania

²Faculty of Science, State University of Zanzibar (SUZA), Zanzibar, Tanzania

Email: abdallamussa@gmail.com, kombokai68@gmail.com, sakhamis3@gmail.com, alfredkondowe@gmail.com, sarah.osima@gmail.com, freemon.king2008@yahoo.com, asyooo@yahoo.com

How to cite this paper: Abdalla, A.H., Kai, K.H., Khamis, S.A., Kondowe, A.L., Osima, S.E., King'uzza, P.H. and Hamad, A.O. (2023) The Influence of Climate Change and Variability on Spatio-Temporal Rainfall and Temperature Distribution in Zanzibar. *Atmospheric and Climate Sciences*, 13, 282-313. <https://doi.org/10.4236/acs.2023.132016>

Received: December 4, 2023

Accepted: April 25, 2023

Published: April 28, 2023

Copyright © 2023 by author(s) and Scientific Research Publishing Inc. This work is licensed under the Creative Commons Attribution International License (CC BY 4.0).

<http://creativecommons.org/licenses/by/4.0/>



Open Access

Abstract

Climate change has resulted in serious social-economic ramifications and extremely catastrophic weather events in the world, Tanzania and Zanzibar in particular, with adaptation being the only option to reduce impacts. The study focuses on the influence of climate change and variability on spatio-temporal rainfall and temperature variability and distribution in Zanzibar. The station observation datasets of rainfall, T_{\max} and T_{\min} acquired from Tanzania Meteorological Authority (TMA) and the Coordinated Regional Climate Downscaling Experiment program (CORDEX) projected datasets from the Regional climate model HIRHAM5 under driving model ICHEC-EC-EARH, for the three periods of 1991-2020 used as baseline (HS), 2021-2050 as near future (NF) and 2051-2080 far future (FF), under two representative concentration pathways (RCP) of 4.5 and 8.5, were used. The long-term observed T_{\max} and T_{\min} were used to produce time series for observing the nature and trends, while the observed rainfall data was used for understanding wet and dry periods, trends and slope (at $p \leq 0.05$) using the Standardized Precipitation Index (SPI) and the Mann Kendall test (MK). Moreover, the Quantum Geographic Information System (QGIS) under the Inverse Distance Weighting (IDW) interpolation techniques were used for mapping the three decades of 1991-2000 (hereafter D1), 2001-2010 (hereafter D2) and 2011-2020 (hereafter D3) to analyze periodical spatial rainfall distribution in Zanzibar. As for the projected datasets the Climate Data Operator Commands (CDO), python scripts and Grid analysis and Display System (GrADS) soft-wares were used to process and display the results of the projected datasets of rainfall, T_{\max} and T_{\min} for the HS, NF and FF, respectively. The results show that the observed T_{\max} increased by the rates of $0.035^{\circ}\text{C yr}^{-1}$ and

0.0169°C yr⁻¹, while the T_{\min} was increased by a rate of 0.064°C yr⁻¹ and 0.104°C yr⁻¹ for Unguja and Pemba, respectively. The temporal distribution of wetness and dryness indices showed a climate shift from near normal to moderate wet during 2005 at Zanzibar Airport, while normal to moderately dry conditions, were observed in Pemba at Matangatuani. The decadal rainfall variability and distributions revealed higher rainfall intensity with an increasing trend and good spatial distribution in D3 from March to May (MAM) and October to December (OND). The projected results for T_{\max} during MAM and OND depicted higher values ranging from 1.7°C - 1.8°C to 1.9°C - 2.0°C and 1.5°C to 2.0°C in FF compared to NF under both RCPs. Also, higher T_{\min} values of 1.12°C - 1.16°C was projected in FF for MAM and OND under both RCPs. Besides, the rainfall projection generally revealed increased rainfall intensity in the range of 0 - 25 mm for Pemba and declined rainfall in the range of 25 - 50 mm in Unguja under both RCPs in perspectives of both NF and FF. Conclusively the study has shown that the under-going climate change has posed a significant impact on both rainfall and temperature spatial and temporal distributions in Zanzibar (Unguja and Pemba), with Unguja being projected to have higher rainfall deficits while increasing rainfall strengths in Pemba. Thus, the study calls for more studies and formulation of effective adaptation, strategies and resilience mechanisms to combat the projected climate change impacts especially in the agricultural sector, water and food security.

Keywords

Climate Change, Climate Variability, Spatial and Temporal Distribution, Temperature, Rainfall, CORDEX

1. Introduction

Climate change is a global phenomenon, with varying indicators and impacts from one region to another. Such indications as noted by the [1] are increasing global air and sea surface temperature, rising sea-level (0.15 - 0.18) m in the 20th century; more frequent heavy precipitation events (rainstorms, floods or snowstorms) in many areas; more intense and longer droughts wider areas, especially in the tropics and subtropics; more frequent and stronger occurrences of hurricane/typhoons and thinning ice caps in the Arctic and Antarctic. Out of those indicators, an extreme increase in global temperature or warming is unequivocal since the 1950s.

The influence of climate change as reported by [2] showed that the number of warm days and nights has increased on a global scale. It is also very likely that human influence has contributed to the observed global-scale changes in the frequency and intensity of daily temperature extremes since the mid-20th century. According to Assessment Report 5 (AR5) of Intergovernmental Panel on Climate Change (IPCC), “global surface temperature changes for the end of the 21st century are likely to exceed 1.5°C relative to 1850-1900 for all RCP except

RCP2.6” [3]. Previously, reference [4] detected a significant increase in temperature, of about 0.15°C per decade over the period 1979-2010 in tropical Africa. This increase of temperature was also consistent with [5] [6] who noted that the magnitude of warming increases from Tanzania’s coastal belt to the interior and northern part of the region. Consequently, high fatality rates were recorded in developing countries because of their high reliance or increasing demands on natural resources and their limited or low coping capacities [7] Additionally, [8] and [3] revealed that the significant consequences of climate change may also result in increased climate variability, reduced crops yield due to changing local temperature regimes and extreme weather events that are likely to decrease the food security of vulnerable populations.

Changes in long-term hydroclimatic variables such as rainfall could represent regional climate change [9] Precipitation can be well explained when they have separated into Inter-annual or temporal and spatial [10] *i.e.* space (geographical variations) trends at regional scales [11] [12] Therefore, understanding the spatial-temporal trends in climate variability, and comprehensive assessments at regional and local scales are fundamental.

The trend in climatic conditions especially rainfall in East Africa is known for its inter-annual variability, which has contributed to the devastating droughts and floods [13] [14] [15]. The reasons for the spatial or temporal trends were explained by [16] who highlighted that variability of rainfall in East Africa, particularly the inter-annual variability, is modulated by large-scale climate forcing and changes in sea surface temperature (SST), which affects the rainfall amount (e.g., decrease during the long-rain season) by changing wind patterns and moisture fluxes. Other studies including [17] [18] [19] and [16] have highlighted that the variability in rainfall in this region is linked to large-scale climate variability and change, not only El-Niño Southern Oscillation (ENSO) but also Indian Ocean Dipole (IOD) and movement of the inter-tropical convergence zone (ITCZ).

In Zanzibar islands, the influence of climate change and variability on spatio-temporal rainfall was well explained by the flood events which forced a significant number of people to migrate their houses, some local bridges to be washed away and strandment of transportation for some time associated with number of observed fatalities [20]. Additionally, frequencies of extreme and severe droughts in Pemba which experienced severe droughts in 1976, 1987 and from 1994-1997 were also detected well during both long and short growing seasons with exception of severe drought events in MAM that lead to changes in forest cover and biomass over time [21] The variability of rainfall has a great impact on agricultural planning and water resources management. For example, rain-fed agriculture has remained the dominant source of staple food production for the majority of rural poor in sub-Saharan Africa [22], for southern, heavy dependence on rain-fed agriculture in Zimbabwe and climate sensitive resources [23] and Zanzibar in particular, where the agricultural activities are rain-fed and about 85% of most of the economic activities depends on the climate-driven

agricultural sector [24].

2. Data and Methods

2.1. Study Sites

Zanzibar is composed of two Islands of Unguja and Pemba, which are situated in the South western Indian Ocean. The geographical location of the islands is roughly defined by grid points ranging from 5.75°S - 6.5°S, and 39.27°E - 39.53°E for Unguja while Pemba is roughly located between 4.93°S - 5.28°S and between 39.67°E - 39.73°E [20] The two sister Islands of Unguja and Pemba are 35 and 56 km off the coast of mainland Tanzania, respectively.

Politically, Zanzibar became a semi-autonomous state under the United Republic of Tanzania (URT) effective in April, 1964. This small Island state has a population of about 1.9 million people [25]. Climatologically, Zanzibar lie under a tropical climate with two distinct rainfall patterns *i.e.* long rains (Masika) which normally start in March and ends in May (MAM) and short rains (Vuli) of October to December (OND) [20] [26]. Reference [27] highlighted that during Masika, the islands are characterized by abundant rainfall with good temporal and spatial coverage, while during Vuli the islands are characterized by limited rainfall anomaly with poor spatial and temporal coverage. Normally the short rains are associated with the northeast monsoon flow, while the long rains are dominated by southerly to southwesterly and southeasterly monsoon flow. Annual and seasonal rainfall rates of Unguja and Pemba, wind pattern (south-east and northeast monsoon), and annual and seasonal temperature rates (maximum, minimum and daily mean). Also [24] has shown that the long-term average maximum temperature during March to May (MAM) season for Zanzibar ranged from 32.4°C for Unguja and 31.6°C for Pemba; while the minimum ranged from 22.7°C and 23.1°C for Unguja and Pemba respectively.

The main socio-economic activities of the people in Zanzibar which form the pillars of its annual Gross Domestic Product (GDP) includes small-scale farming, tourism, business as well as fishing [28]. Other activities that contribute to GDP in Zanzibar are sand mining and other sectors of blue economy in the islands. The details of the study region are shown in **Figure 1**.

2.2. Datasets

The study used two types of datasets, namely the station's observation data and the CORDEX model simulated or projected data. The station observation datasets include the maximum (T_{\max}) and minimum (T_{\min}) temperature records, and the monthly observed rainfall with temporal coverage of 30 years (1991-2020) from the nine (9) stations with details depicted in **Table 1**. These data were acquired from TMA, Zanzibar office. The rainfall station observation datasets were used for the analysis of SPI, Mann Kendall test as well and the decadal spatial distribution of rainfall, while the observed temperatures were used to generate the long term series for observing the nature and its trend. The model simulation

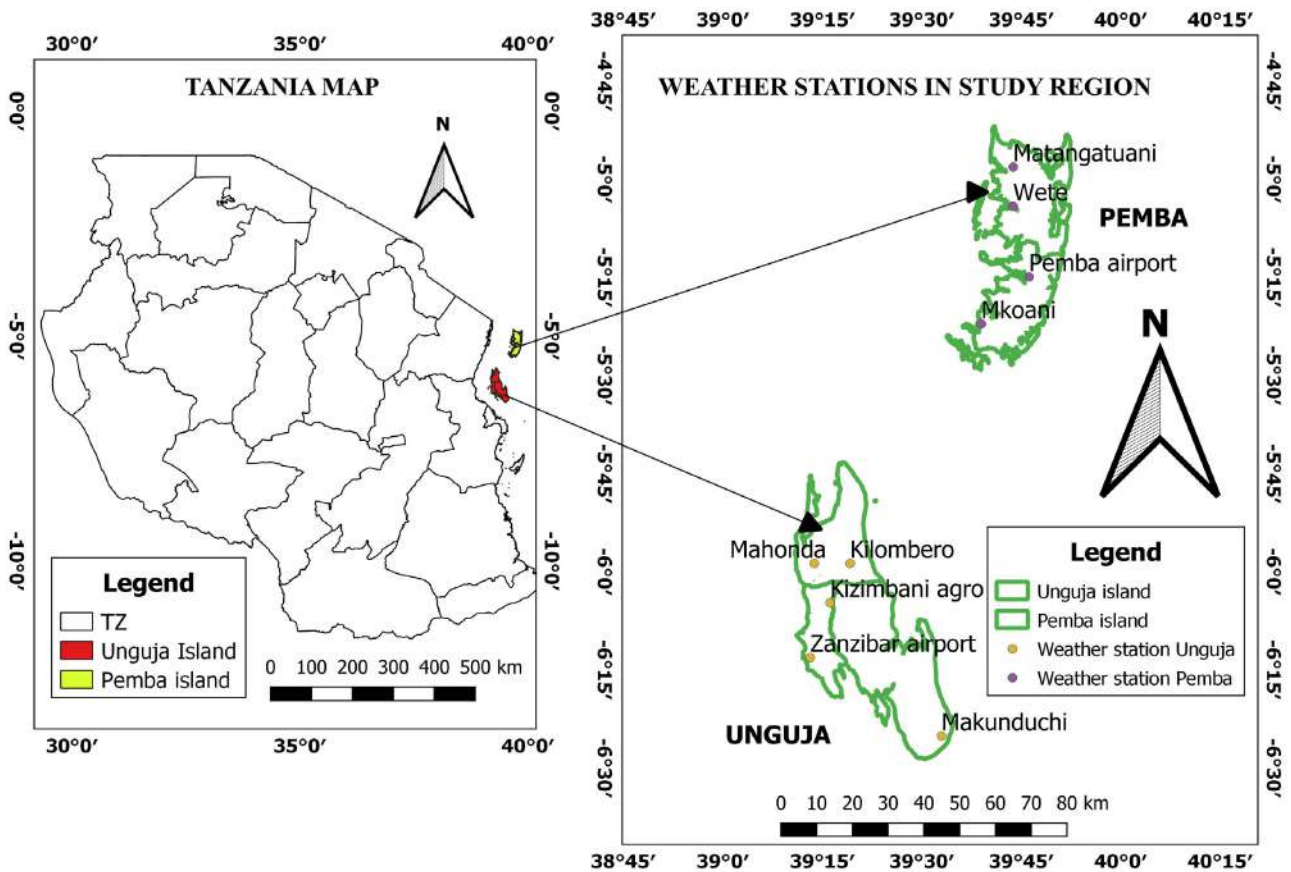


Figure 1. Study area: source (GIS Tanzania administration layer freely downloaded in internet).

Table 1. Standardized precipitation index (SPI) thresholds and their descriptions.

SPI Value	Meaning
2.0+	Extremely wet
1.5 to 1.99	Very wet
1.0 to 1.49	Moderately wet
-0.99 to 0.99	Near normal
-1.0 to -1.49	Moderate dry
-1.5 to -1.99	Severe dry
-2 and less	Extremely dry

or projected datasets were customized to longitude 0.44° and latitude 0.44° using rotated pole system coordinates of the Regional Climate Model (CORDEX). The acquired model datasets include the projected T_{max} (tas_{max}), T_{min} (tas_{min}) and precipitation (pr), which were downloaded from the registered CODEX links of <https://climate4impact.eu/impactportal/general/index.jsp> and <https://esgf-data.dkrz.de/projects/esgf-dkrz/>, respectively. These datasets were downloaded using two RCPs of 4.5 and 8.5. The CORDEX downloaded datasets were of three categories namely 1) historical datasets with temporal coverage of 1991-2005 2) The projected datasets with temporal coverage of 2006-2100 using climate data operators (CDO).

2.3. Methods

2.3.1. Trend Analysis

The station observation data were processed and tested for homogeneity using the interpolations methods including arithmetic mean among others. The standardized precipitation index (SPI) from different stations in Zanzibar were calculated and plotted in time series to show the period of wet and dry conditions based on descriptions in **Table 1** [29] [30] and was used to classify the wet and dry conditions using the thresholds presented in **Table 1**.

2.3.2. Mann Kendall Test

The Mann-Kendall (MK) trend test is a non-parametric statistical method used to capture data trends over time [31] [32]. The test observes whether a random response variable monotonically rises or falls with time [33]. The standardized Mann Kendall test is given by equation

$$S = \sum_{k=1}^{n-1} \sum_{j=k+1}^n \text{sign}(x_j - x_k) \quad (1)$$

where S is a statistic, k , are the sequential data values, and is the distance of the time series, where $\text{sign}(x_j - x_k)$ is well explained by [34] in the Equation (2).

$$\text{Sign}(x_j - x_k) = \begin{cases} 1 & \text{if } x_j > x_k \\ 0 & \text{if } x_j = x_k \\ -1 & \text{if } x_j < x_k \end{cases} \quad (2)$$

where $\text{Sign}(x_j - x_k) = 1$ if $(x_j - x_k) > 0$; $\text{Sign}(x_j - x_k) = 0$ if $(x_j - x_k) = 0$ and $\text{Sign}(x_j - x_k) = -1$ if $(x_j - x_k) < 0$.

$$\text{When } n \geq 10 \quad (3)$$

Statistic S is approximately normally distributed [35]

In the monotonic trend test, the null hypothesis (H_0) is referred as the data have no trend and its alternative hypothesis (H_1), indicates a rise or fall in a monotonic trend [36], where positive (+) values specify a rise over time while negative (-) values indicate descend. Since the data is independent and normally distributed, the variance of the S statistic ($\text{Var}(S)$) is

Identified by;

$$\text{Var}(S) = \frac{n(n-1)(2n+5)}{18} \quad (4)$$

The test statistic Z is computed using the values of $\text{VAR}(S)$ and S [37] [38] [39]

$$Z = \begin{cases} \frac{S-1}{\sqrt{\text{Var}(S)}} & \text{if } S > 0 \\ 0 & \text{if } S = 0 \\ \frac{S+1}{\sqrt{\text{Var}(S)}} & \text{if } S < 0 \end{cases} \quad (5)$$

[34] revealed that statistically significant trends are calculated by the Z val-

ue, where positive value represents increasing variation (rising trend) and the negative value decreasing variation or fall trend [32]. The null hypothesis is rejected at the significance level if $|| \geq /2$, where $/2$ is the critical value of the standard normal distribution with a probability exceeding $/2$, and it shows that the trend is significant. If $|| < Z_{\alpha/2}$ the null hypothesis is recognized, and the trend is not significant. A trend is examined to be statistically significant at the 0.05 level [34].

The Sein's slope estimator under the non-parametric method to estimate the true slope of an existing trend that is a change per year [40] [41]. The Sein's method is mostly used in cases where the trend is assumed to be linear and is used under a simple non parametric procedure [42]. This means that linear model $f(t)$ can be described as

$$f(t) = Qt + B \quad (6)$$

The $f(t)$ is defined as a function of time which represents the time series, whereby it can be increasing or decreasing, t is the date (time) values, B is a constant and Q is the slope as explained by [32] [39] in the Equation (7)

$$Q_i = \frac{x_j - x_k}{j - k} \quad (7)$$

Also [39] note that at time, $j > k$ and $i = 1, 2, \dots, N$, the values of the data pairs are represented by x_j and x_k . The median of the N values of Q_i can be determined as

$$Q_{med} = \begin{cases} Q_{(N+1)/2} & \text{if } N \text{ is an odd number} \\ \frac{Q_{(N/2)} + Q_{(N+1/2)}}{2} & \text{if } N \text{ is an even number} \end{cases} \quad (8)$$

An increasing trend can be discerned when the value of Q_i is positive, and a decreasing trend if the value of Q_i is negative. There is no trend when Q_i is zero.

2.3.3. Rainfall Spatial Distribution for Three Decades

The Geographic Information System (GIS) is a computer system that analyzes and displays geographically referenced information. It combines software tools for managing, analyzing, editing and visualizing such information [43] [44]. Quantum GIS (QGIS), a free and open-source software were used to produce the spatial rainfall patterns using the Inverse Distance Weighting (IDW) interpolation. IDW is the simplest interpolation method whereby a neighborhood for the interpolated point is identified and a weighted average is taken within this neighborhood. The weights are always observed to show it as a decreasing function of distance expressed as or a number of points or a radius [45] [46]. The interpolated rasters were plotted in annual as well as seasonal scales of (MAM and OND) in ten years (decade) intervals. The decadal differences in raster format were also calculated and plotted.

2.3.4. Processing and Analyzing the CORDEX Data

As for CORDEX data, CDO commands include (cdo merge time, sellonlatbox,

selmon among others) were used to navigate the downloaded netcdf (.nc) files of rainfall (pr), T_{\max} (tas_{max}), and T_{\min} (tas_{min}) and then calculate these parameters in seasonal (MAM and OND) averages for both RCPs (*i.e.* 4.5 and 8.5) and for all three time slices. The HS datasets were used as a reference climatology to calculate the NF and FF departures (anomalies) for both RCPs (4.5 and 8.5). Using the sellonlatbox CDO commands the CORDEX were customized to captured the two island of Unguja and Pemba using the grid boxes of 4.8S to 6.6S and 39.1E to 40.0E. The customized datasets for Zanzibar were visualized using free source open GrADS software. The processed datasets were analyzed and plotted to project the NF and FF projections of the rainfall and temperatures of Zanzibar for the two RCPs of 4.5 and 8.5, respectively.

3. Results

3.1. Standardized Precipitation Index (SPI)

The results of the SPI presented in **Figure 2(a)** revealed that Zanzibar Airport

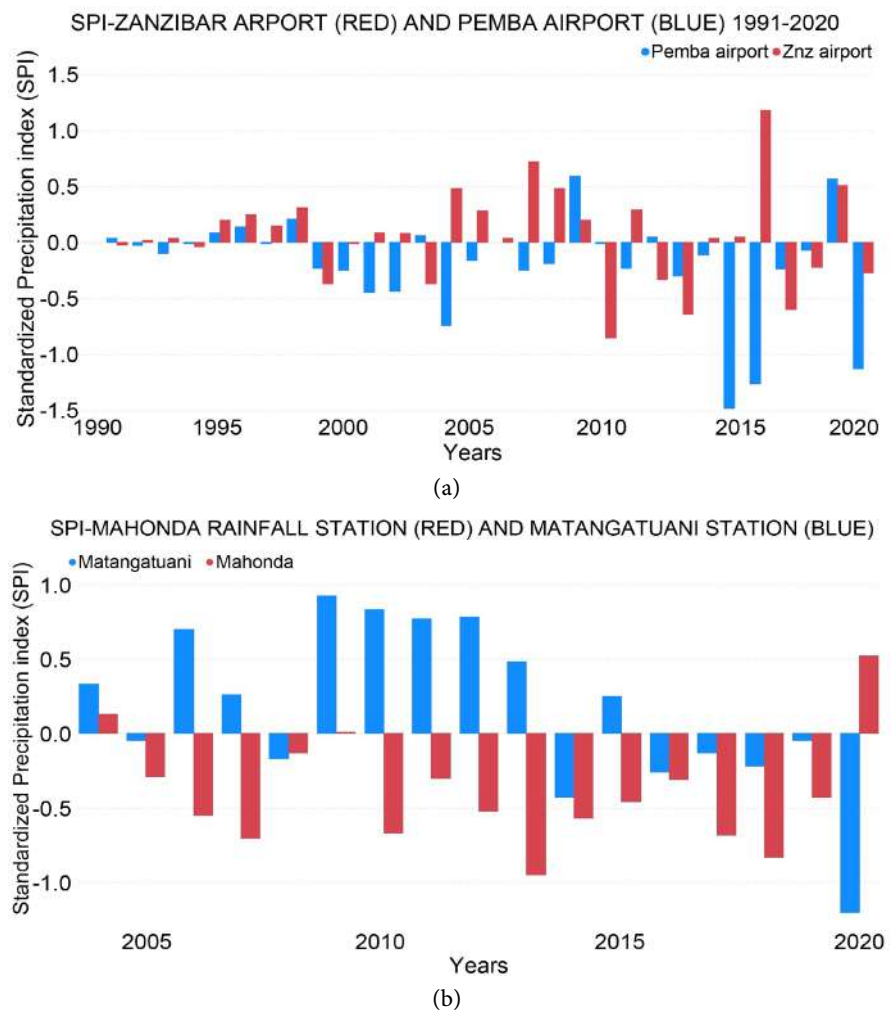


Figure 2. (a) Upper panel SPI for Zanzibar Airport (red) and Pemba Airport (blue); (b) Lower panel similar to (a) but for Mahonda rainfall (red) and Matangatuani (blue).

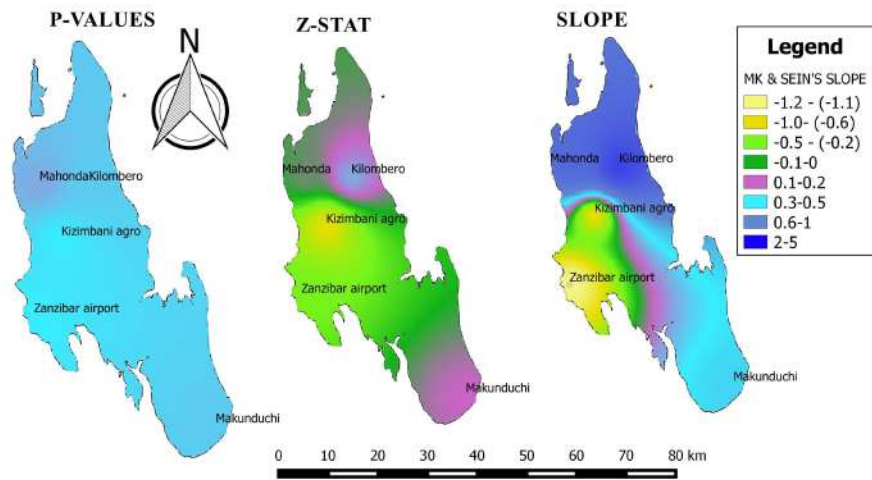
have a positive SPI of near normal from 1991 to 1998, with moderate wet conditions during 2004-2009. The SPI for Pemba showed near normal conditions to moderately dry up to 2004, while moderately dry condition from 2015 onward with exception of 2019 which was normal to near normal. The dry and wet periods results in Mahonda (Unguja) and Matangatuani (Pemba) presented in **Figure 2(b)** show that Mahonda station was dominated by negative SPI which indicates near normal to moderate dry conditions except for 2004 and 2020, while the inter-annual variability of wet and dry conditions for Matangatuani shows that the station was mostly dominated by moderately wet condition from 2006-2013, and near normal to moderately dry condition from 2016 onward, indicating that the existing climate change has resulted in declining rainfall at Matangatuani, especially over the last ten years.

3.2. Mann Kendall Test and Sein's Slope Results

The results of the Mann Kendall's (MK) test and Sein's slope at $p = 0.05$ and under H_0 that there is no significant trend in rainfall distribution in Zanzibar presented in **Figure 3** show that Unguja and Pemba islands (**Figure 3(a)** and **Figure 3(b)**), had $p > 0.05$ which depicted an increasing monotonic and thus rejecting the stated H_0 and accepting the H_1 . Also **Figure 3(a)** (left panel) reveals that the intensity of p values was highest at urban west region of Unguja as compared to the northern and southern regions, indicating that the urban west region and its nearby areas are experiencing higher rainfall than the Northern and Southern parts of Unguja. As for Pemba, p values is highest at the northern part of Pemba compared to the southern. **Figure 3(b)** (left panel) indicating higher rainfall at Matangatuani and Wete compared to the rest. Also, the results in **Figure 3(a)** are in agreement with **Figure 2(b)** that Mahonda station in Unguja has weak rainfall intensity as well as weak monotonic rainfall trend though significant. The results of the Z statistics for Unguja island (**Figure 3(a)** middle panel) shows that the northern and southern part have positive z values indicating positive trend and the central part of the island depicts negative trend. The results of the Sein's slope for the Unguja island (**Figure 3(a)** right panel) shows that the magnitude of rainfall is less than 1 mm per month for central region Unguja. It is slightly increasing (positive slope) over southern part and significantly increasing to the rate of +2.7 mm/months over the urban west and to northern part of Unguja island.

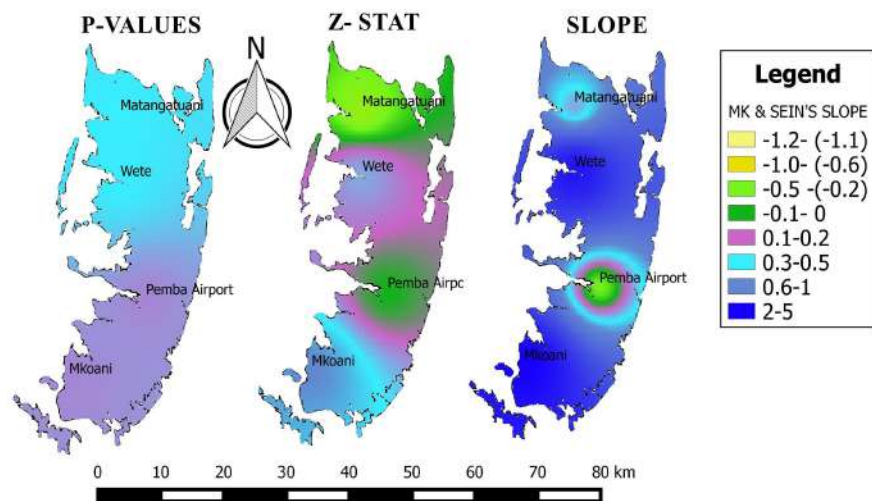
As for Pemba, results in **Figure 3(b)** is in agreement with the results presented in **Figure 2** which shows that the inter-annual variability of the wet and dry values (SPI) was mostly wet condition over Matangatuani Pemba. The results of the Z statistics (**Figure 3(b)** middle panel) shows that the southern part have positive z values indicating positive trend while Matangatuani depicts negative trend. As for the sein's slope's result in **Figure 3(b)** (lower right panel) shows that the slope shift from negative to positive at Pemba Airport and the Western Matangatuani, but the slope was slightly increasing at Wete and significantly increasing at Mkoani which indicating that Mkoani receives large

MANN KENDALL AND SEIN'S SLOPE RESULTS-UNGUJA



(a)

MANN KENDALL AND SEIN'S SLOPE RESULTS-PEMBA



(b)

Figure 3. (a) Upper panel Mann Kendall and Sein's slope test results for Unguja; (b) Lower panel Mann Kendall test and Sein's slope test results for Pemba.

amount rainfall compared to other regions.

3.3. Analysis of Temperature Trends

The results of analysis of the T_{\max} for Zanzibar airport for the period of last thirty years (1991-2020) presented in **Figure 4** shows that the rate of change of T_{\max} was $0.035^{\circ}\text{C}/\text{yr}$. Further results in **Figure 4** show that the period from 1991 to 2009 was characterized by negative T_{\max} anomalies indicating cold conditions, while from 2005 onwards the results show the dominance of positive T_{\max} anomalies indicating increasing in warm conditions as well as a climate shift since 2005 onwards. This finding is well agreed by the [2] which indicates that in the

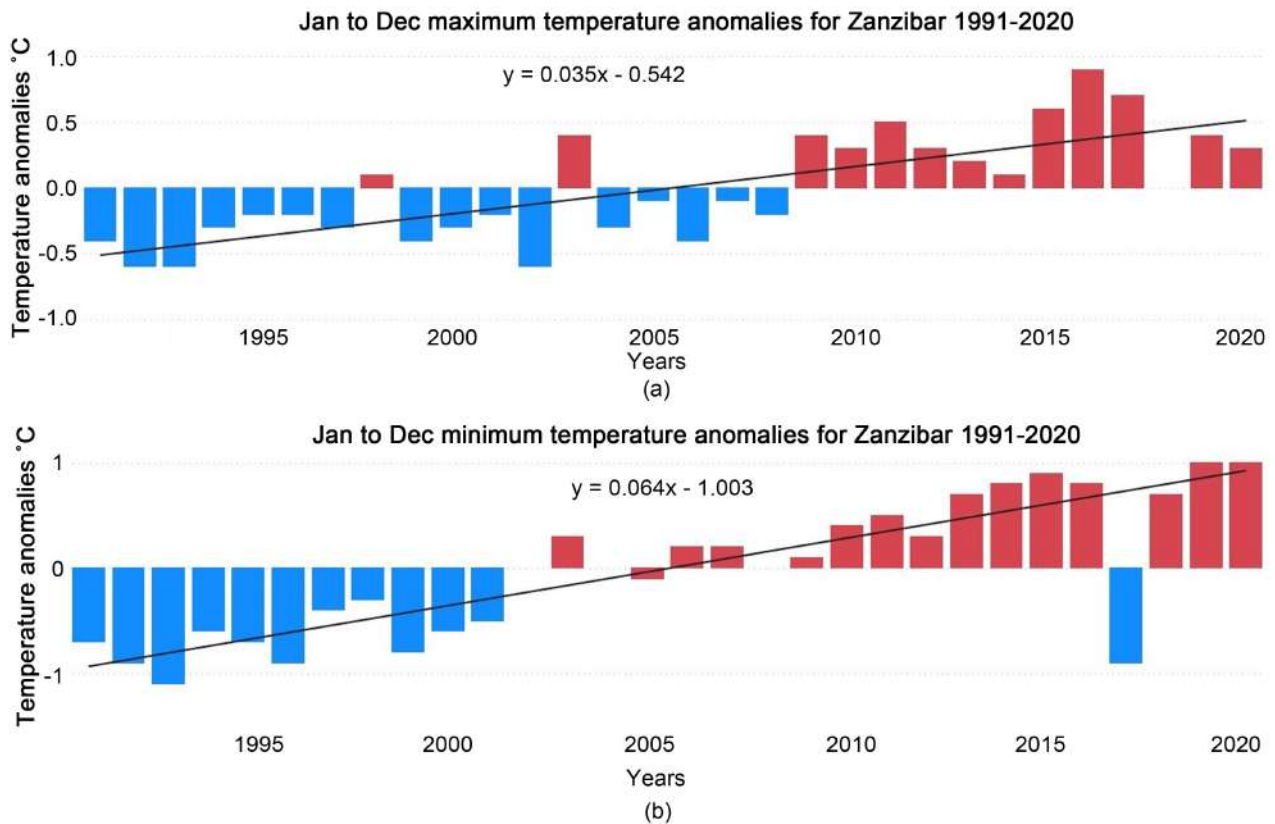


Figure 4. Maximum (T_{\max}) and Minimum (T_{\min}) temperature anomalies-Unguja.

last decade of 20th century and the first decades of the 21st century are the warmest periods. On the other hand, results in **Figure 4(b)** revealed that the rate of change of minimum temperature was $0.064^{\circ}\text{C}/\text{yr}$ which is approximately twice that of T_{\max} indicating an increase in warming nights. Also like T_{\max} , the inter-annual variability of T_{\min} revealed negative anomalies i.e. cold condition (nights) for the period running from 1991 to 2001 with shifting to positive anomaly in 2002. Moreover, **Figure 4(b)** shows that effective from 2003 to 2020 except 2017 the T_{\min} anomalies were positive increasing indicating a decreasing rate and strength of cold nights. This trend of T_{\min} positive increasing could be well agreed by [47] that there is increasing trend in the percentage of warm nights including Zanzibar. Also these findings are well agreed by the [2] which noted that the T_{\min} was increased very rapid compared to T_{\max} due to increased Green House Gases (GHGs), aerosol among others.

The rate of change of T_{\max} for Pemba island for 1991-2020 presented in **Figure 5(a)** is $0.0169^{\circ}\text{C}/\text{yr}$ which represents a positive trend and daily to monthly warming condition. T_{\max} negative anomaly occurs from 1991 to 2006 except for 1995, 1998, 2003 and 2004. Besides **Figure 5** shows a climate shift in 2005 and the positive T_{\max} anomalies were depicted from 2008 to 2020 with the exception of 2008, 2012 2019 and 2020. T_{\min} for Pemba reveals an increasing trend of $0.104^{\circ}\text{C}/\text{yr}$ (**Figure 5(b)**) indicating an increase of warming. The presented

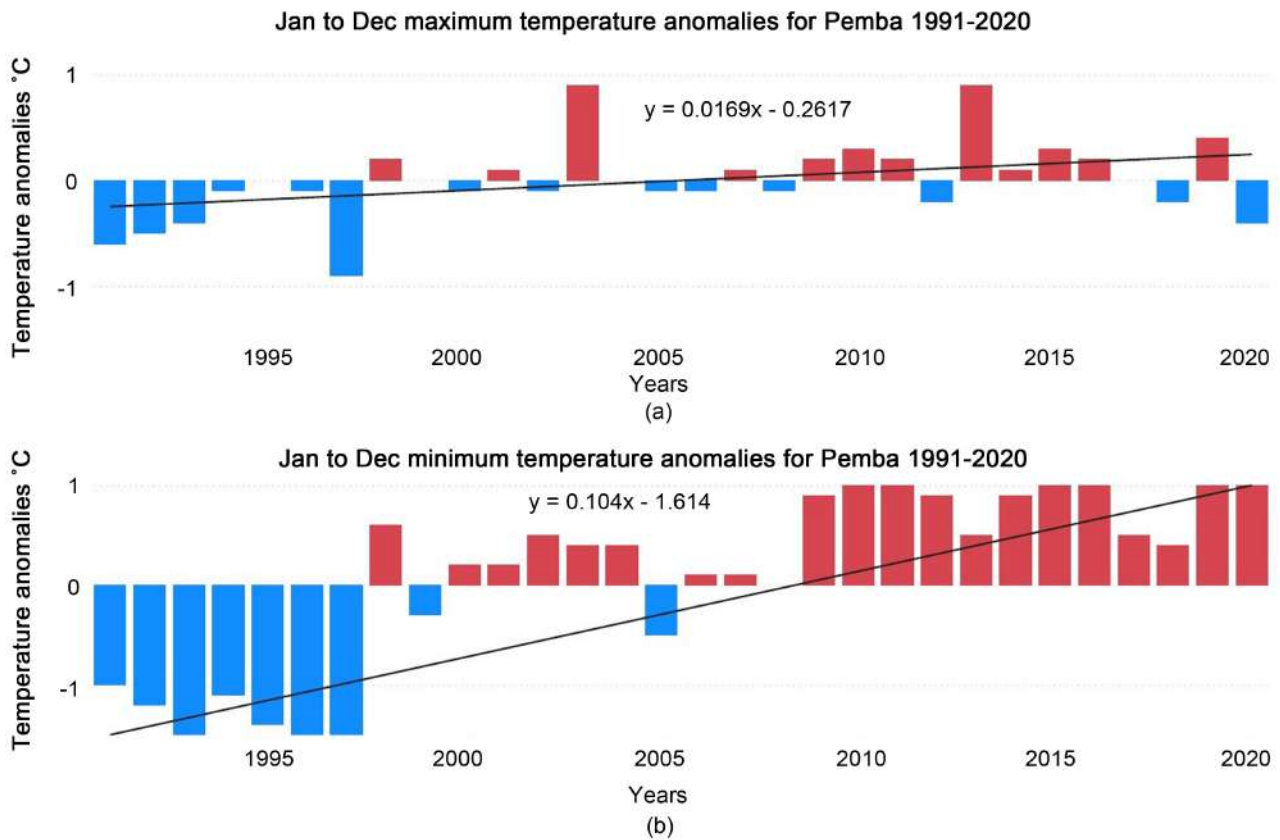


Figure 5. Maximum (T_{\max}) and minimum (T_{\min}) temperature anomalies-Pemba.

negative T_{\min} anomalies during 1991 to 1997 represent a cold condition. Also, **Figure 5(b)** shows the positive T_{\min} anomalies from 1998 to 2020 with the exception of 1999 and 2005. This progression of positive T_{\min} anomalies for about 24 years could be attributed to the influence of climate change, as agreed by the IPCC report that the first decade of the 21st century to be among the warmest periods in history. These results is agreed with [47] who noted that the increasing trend in the percentage of warm days and warm nights are mostly depicted over the eastern parts of the country including Zanzibar, Dar-es-Salaam, Mtwara, and Mbeya regions and areas around Kilimanjaro.

3.4. March to May Rainfall Distribution in Unguja and Pemba

The results of the spatial rainfall distribution for the three decades of 1991-2020 (hereafter D1); 2001-2010 (hereafter D2); and 2011-2020 (hereafter D3) for the MAM period in Unguja are presented in **Figure 6(a)** (upper panel). The MAM rainfall distribution during D1 (**Figure 6(a)**) show the highest peaks ranged at 805 - 999 mm at Urban west region (Kizimbani and Zanzibar airport stations) followed by the Southern region (Makuduchi and the nearby stations) and the lowest rainfall strength occurred at northern region of the island at a range 0 - 599 mm. These results indicate that for D1 the northern region was experiencing drier conditions. The results for D2 shows the rainfall strength at the northern

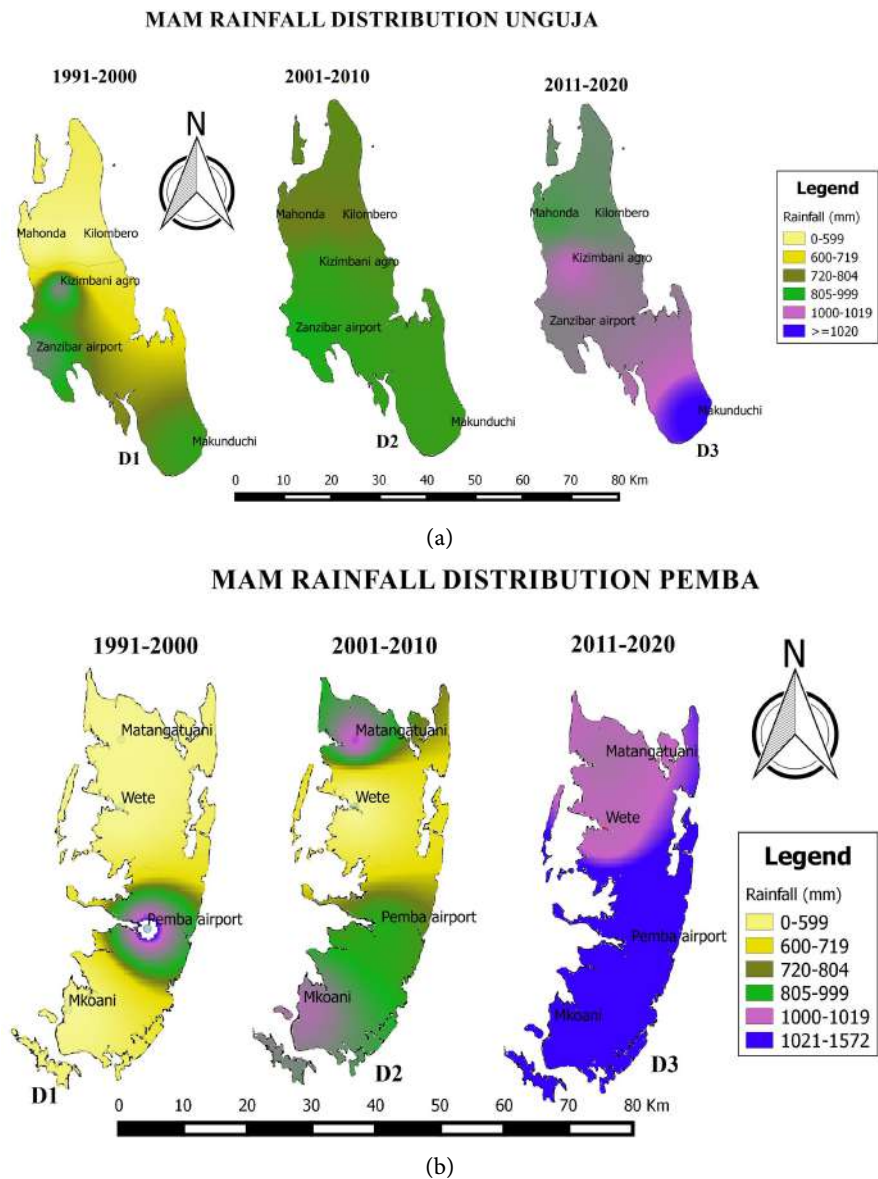


Figure 6. (a) Upper pannel MAM rainfall distribution in Unguja; (b) Lower pannel MAM rainfall distribution in Pemba.

part of the island and the similar coverage at the Urban west region as D1 concentrated only in the west B district. Unlike the periods D1 and D2, the rainfall distribution in D3 shows that the highest rainfall ranged with greater than 1020 mm was distributed at the southern region, while moderate rainfall ranged from 1000 - 1019 mm was mapped at the Urban west and the least rainfall 700 - 804 mm was mapped at the northern region. These results show the shift of rainfall distribution from the highest at Urban west to the southern region of Unguja. Also **Figure 6(a)** shows that D3 has the highest rainfall intensities than D1 and D2 indicating that the last decade of the 20th and the first two decades of the 21st century have revealed higher rainfall intensities in Unguja during the MAM period, but these rainfalls show poor spatial distribution. Further results in **Fig-**

Figure 6(a) reveals the dryness of the northern region for last 30 years. The results of the MAM spatial rainfall distribution for Pemba island presented in Figure 6(b) (lower panel) shows significant changes of the rainfall distribution from D1 to D3. The spatial rainfall distribution in D2 (Figure 6(b)) has shown significant shift of rainfall distribution with the highest rainfall ranged from 805 - 999 mm mapped at the northern tip (Matangatuani station) and the southern tip (Mkoani) compared to 720 - 804 mm in D1. In general, the spatial distribution of MAM rainfall in Pemba (Figure 6(b)) shows a significant increase of MAM rainfall over the southern part of the island (Mkoani) D2 to D3 with an average rainfall intensity of up to 1572 mm in D3. Through these results, one can conclude that climate change has resulted into MAM rainfall shift over Unguja island as well as the existing variability and shifts of rainfall intensities from D1 to D3 could be associated with the climate change and variability in Pemba.

3.5. October to December (OND) Rainfall Distribution at Unguja and Pemba

The results of the spatial rainfall distribution in Unguja during OND presented in Figure 7(a) (upper panel) shows slight changes or shifts from D1 to D3 with higher rainfall intensities mapped at the Urban west region for all decades (D1 to D3), and slight changes of 250 - 399 mm at southern region during D1 to low rainfall intensity during D3. Like the MAM season, the rainfall intensity during D3 is higher than that during D1 and D2 indicating that the second decade of the 21st century to be characterized by higher rainfall intensities in most areas of Unguja. Further results in Figure 7(a) show persistent peaks for all periods (D1 to D3) which were centered at Kizimbani agromet and Zanzibar airport.

As for Pemba, the results of the climate change influence on spatial rainfall distribution revealed significant increase of rainfall intensity at Chake-Chake district during D1 (Figure 7(b) lower) with low rainfall intensities mapped at northern (Wete district and Micheweni district (Matangatuani)) and the southern region at Mkoani district. As for D2 results in Figure 7(b) shows the significant shift of rainfall distribution mapped with higher intensities ranged from 400 - 499 mm with the exception of Wete district which was mapped with very low rainfall (0 - 99 mm). The results in D3 (Figure 7(b)) shows a significant shift of the rainfall intensity with Mkoani leading with higher intensity (568 - 641 mm) compared to low in all northern and southern districts of Wete, Micheweni and Chake - Chake. Like in Unguja Island the spatial rainfall distribution during D3 has mapped with higher intensities D1 and D2, also results has persistently shown that Wete district is characterized with low OND rainfall through all three periods (D1-D3). The increase in rainfall intensity during D3 could be explained by the fact that the increased frequency of the severe weather events which induced the extreme wetness of the three consecutive seasons of MAM, 2019, OND, 2019 and JF (2020) of seasonal rainfall as concurred with [20] [24].

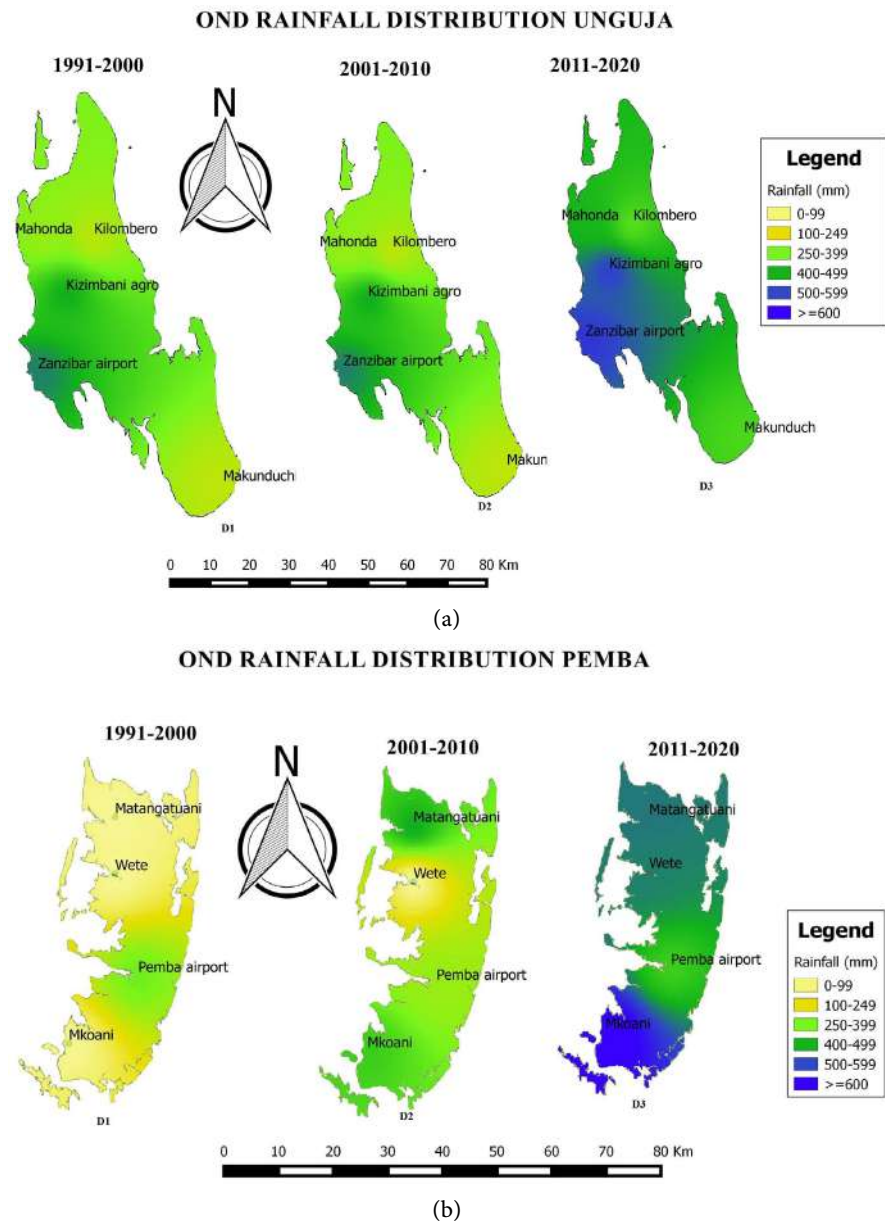


Figure 7. (a) Upper panel OND rainfall distribution in Unguja; (b) Lower panel OND rainfall distribution in Pemba.

3.6. Annual Rainfall Distribution in Unguja and Pemba

The distribution of annual rainfall in Unguja shows the increase from first (Figure 8 upper panel D1) to the second decade (D2) and significant to the third decade over the northern part of the island. Significant distribution of annual rainfall from Kizimbani, Zanzibar airport and part of central Unguja D1 to D3. The southern part seems to maintain the distribution of the average rainfall for two decades followed by a slight increase in rainfall, especially at Makunduchi in which rainfall over the southern part is influenced by climate variability. The results of the influence of climate change on the annual rainfall distribution at Pemba presented in Figure 8(b) revealed that during D1 only central Pemba

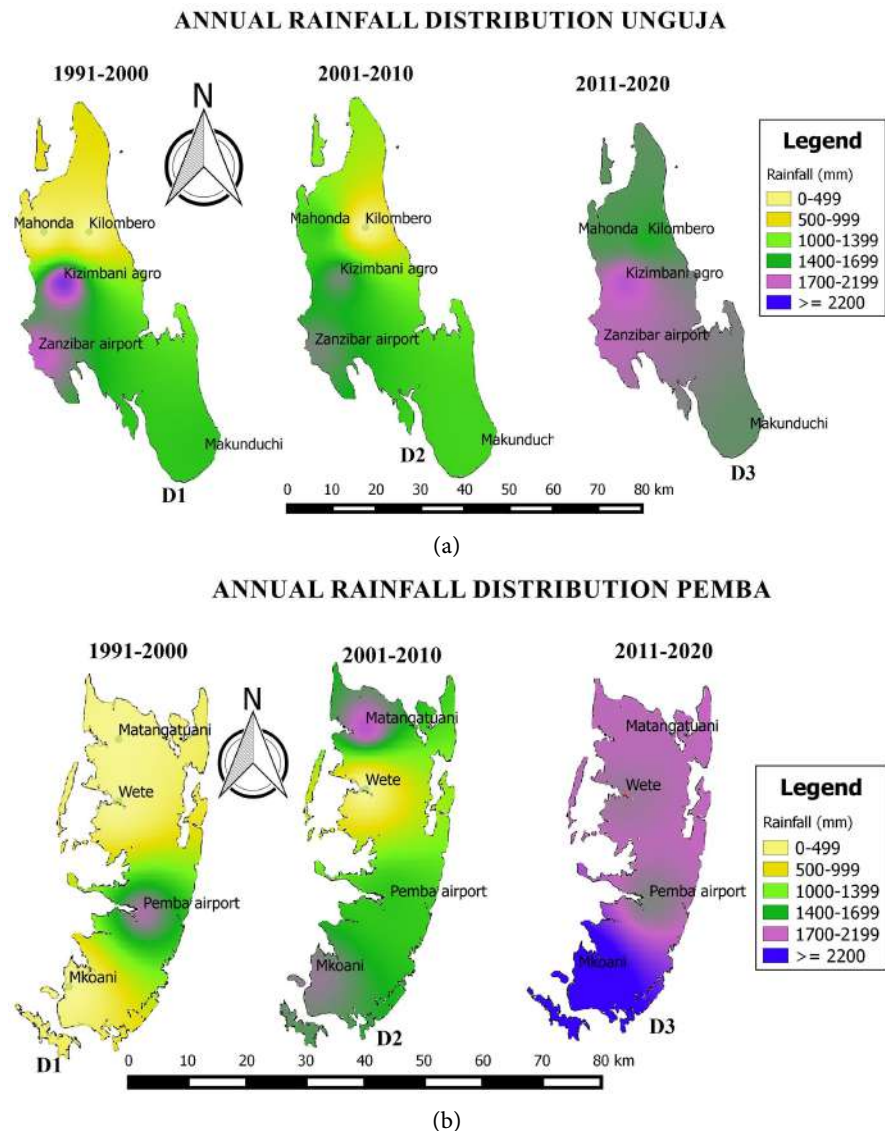


Figure 8. (a) Upper pannel Annual rainfall distribution in Unguja; (b) Lower pannel Annual rainfall distribution in Pemba.

(Chake-Chake district) was characterized by high rainfall intensity ranging from 1400 - 1700 mm, while the southern and northern Pemba was mapped with low rainfall intensity ranging from 0 - 500 mm. The mapped rainfall intensities during D2 presented in **Figure 8(b)** revealed a reverse in rainfall intensities with the tips of northern and southern Pemba having high rainfall intensity compared to the central, and Wete districts being mapped with low rainfall intensity. The results in D3 **Figure 8(b)** show that unlike D1 and D2, the annual rainfall distribution has highly changed with higher intensities mapped over the southern tip of Pemba island (Mkoani) and the remaining parts *i.e.* Wete and Chake-Chake districts being mapped with moderate to low rainfall intensities. These results in D1 to D3 have shown the rainfall shifting due to the influence of climate change with D3 having affected the rainfall intensity in most areas in

Pemba island.

3.7. March-May and October-December Rainfall Projection under RCP 4.5 and RCP 8.5

The projected rainfall results for the NF, and FF with respect to historical (HS) have shown that, MAM rainfall projection under RCP 4.5 (**Figure 9**) and RCP 8.5 **Figure 10** that Unguja and Pemba islands are in decreasing rainfall in the range of 0 - 25 mm NF and increasing in the range of 25 - 50 mm Unguja and 0 - 25 mm in Pemba during FF. Also, results have shown that under RCP 8.5, Unguja and Pemba are characterized by decreasing/increasing rainfall (by a range of 25 mm) in the NF, and vice versa for the FF. As for OND rainfall, the presented projection under RCP 4.5 and RCP 8.5 **Figure 11** and **Figure 12** revealed a decreasing rainfall in Unguja at a range of 25 - 50 mm for both NF and FF, while Pemba will be characterized by an increasing rainfall of 0 - 25 mm for FF under both RCPs, while increasing/decreasing at the same under RCP 8.5/4.5 in NF (**Table 2**). The study results are in agreement/disagreement with [48] for Pemba and Unguja under both RCPs and both time periods (NF and FF).

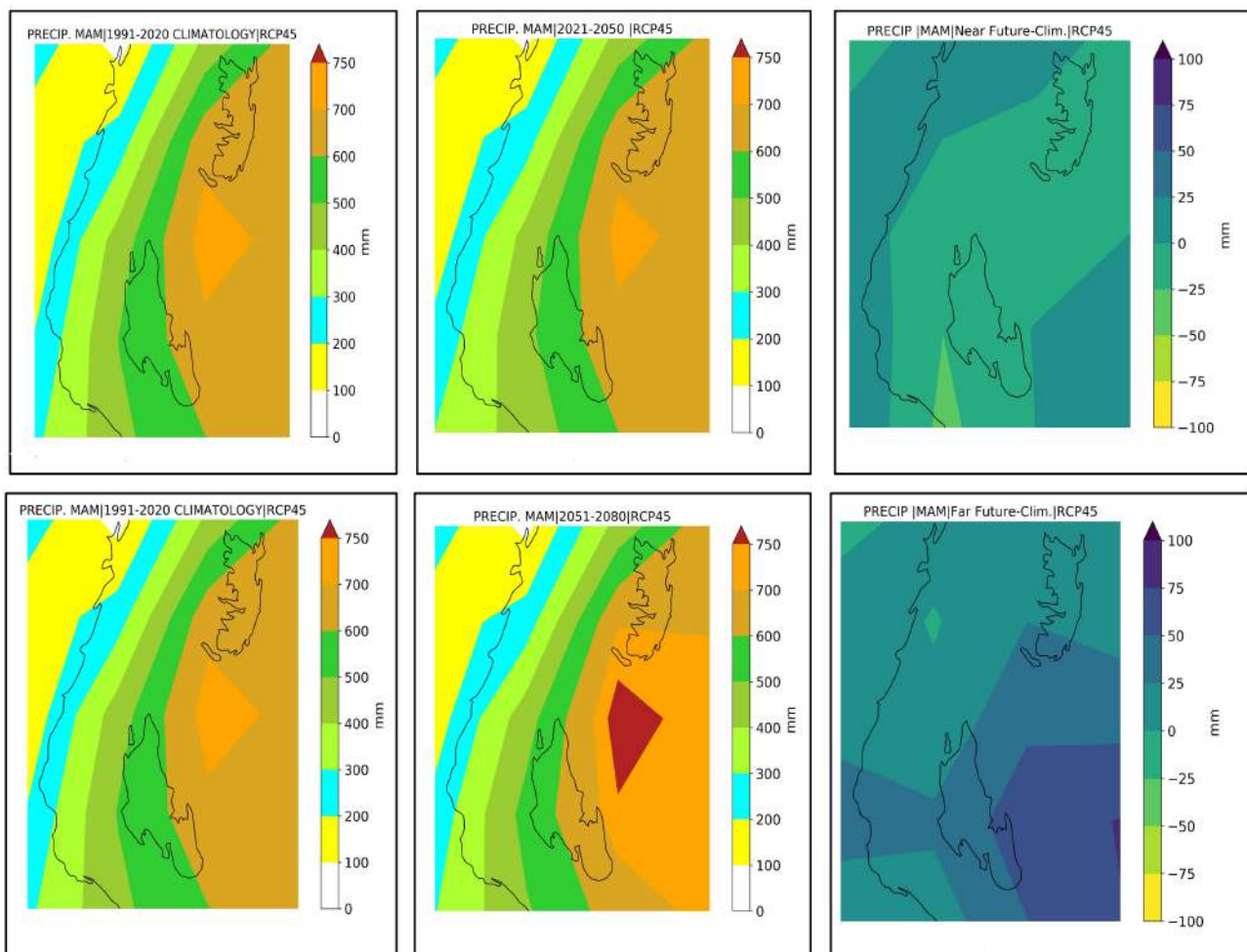


Figure 9. MAM precipitation under RCP 4.5, near future (upper) and far future (lower) and the departures.

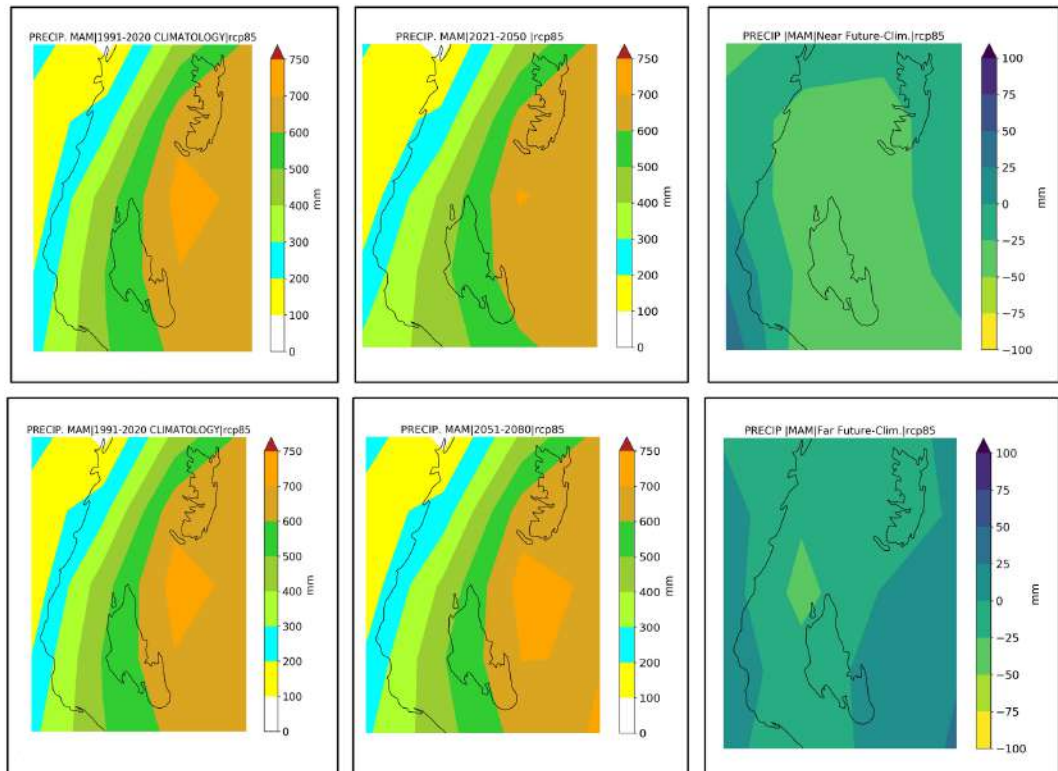


Figure 10. MAM precipitation (mm) under RCP 8.5, near future (upper) and far future (lower) and the departures.

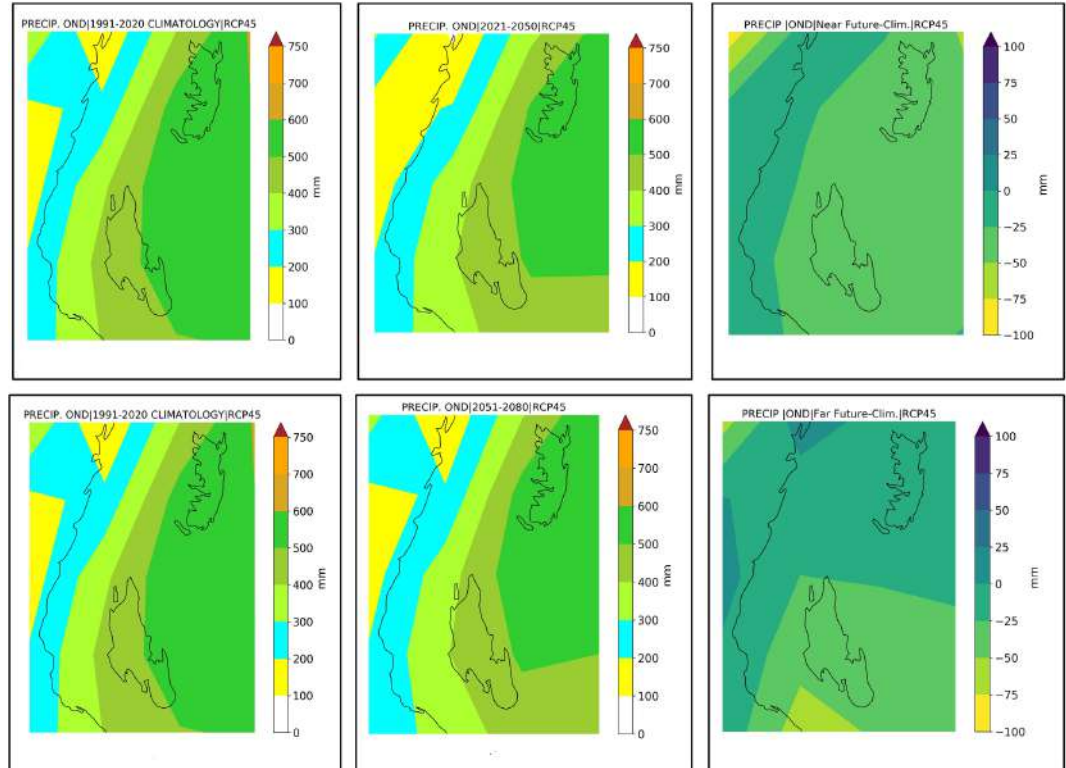


Figure 11. OND precipitation (mm) under RCP 4.5, near future (upper) and far future (lower) and the departures.

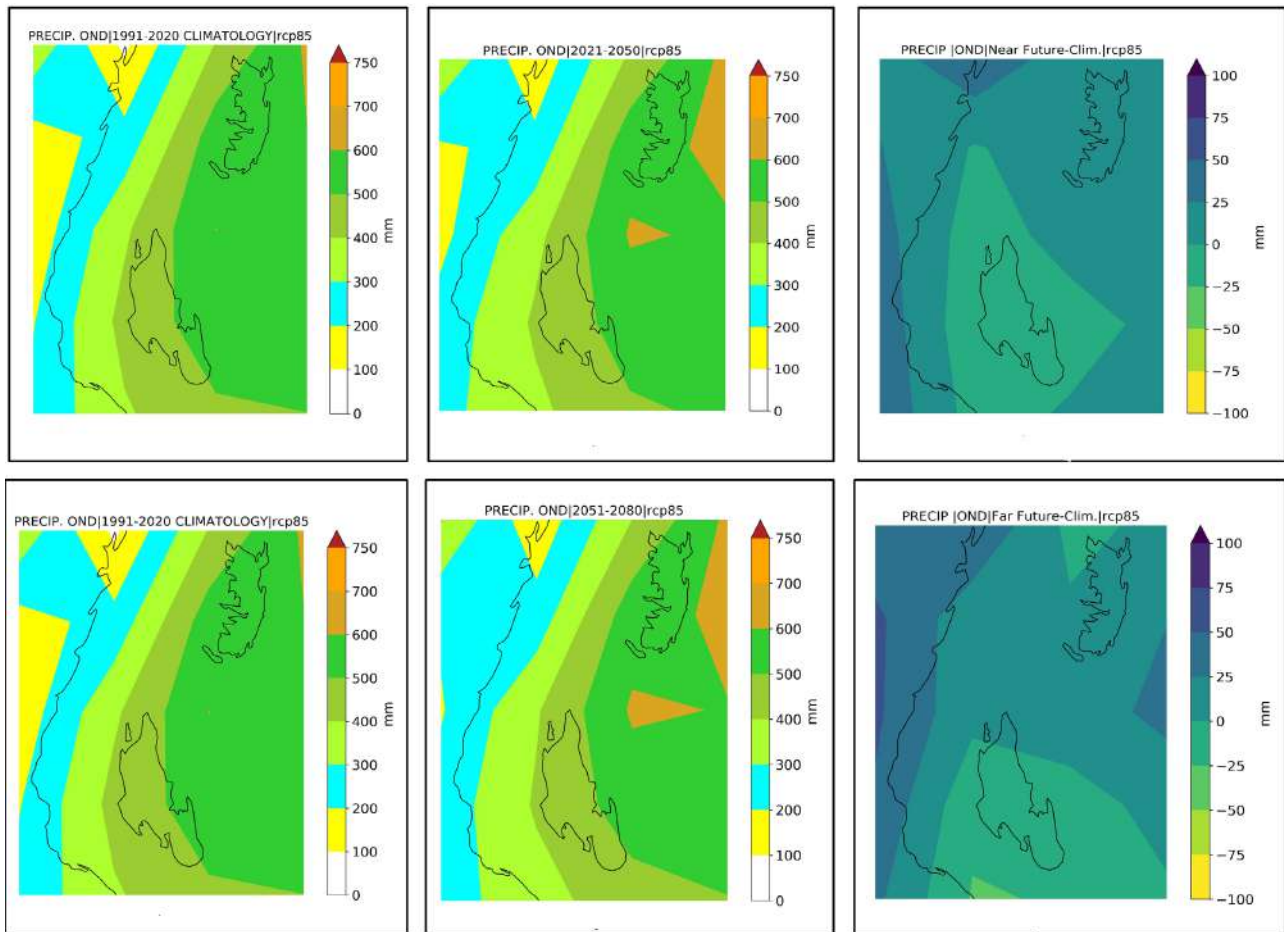


Figure 12. OND precipitation under RCP 8.5, near future (upper) and far future (lower) and the departures.

Table 2. The summarized results of MAM and OND seasonal rainfall projection under RCP 4.5 and RCP 8.5 in Unguja and Pemba Islands.

Parameter: Rainfall (mm)	RCP 4.5				RCP 8.5			
	MAM season		OND season		MAM season		OND season	
	NF	FF	NF	FF	NF	FF	NF	FF
UNGUJA	decreasing from 0 - 25	increasing from 25 - 50	decreasing from 25 - 50	decreasing from 25 - 50	decreasing from 25 - 50	increasing from 0 - 25	decreasing from 25 - 50	decreasing from 25 - 50
PEMBA	decreasing from 0 - 25	increasing from 0 - 25	decreasing from 25 - 50	increasing from 0 - 25	increasing from 0 - 25	decreasing from 0 - 25	increasing from 0 - 25	increasing from 0 - 25

3.8. The Projections of March to May and October-December Maximum Temperature Variation under RCP 4.5 and RCP 8.5

Results of the projected mean T_{max} under RCP 4.5 and RCP 8.5 presented in **Figure 13** and **Figure 14**; Upper left and middle; lower left panel show that the mean T_{max} during MAM is projected to increase with time from the range of 27°C - 27.5°C (HS) to 27.5°C - 28.0°C (NF); 29.5°C (FF) for both Unguja and Pemba. FF in MAM season depicted higher T_{max} under RCP 4.5 and RCP 8.5

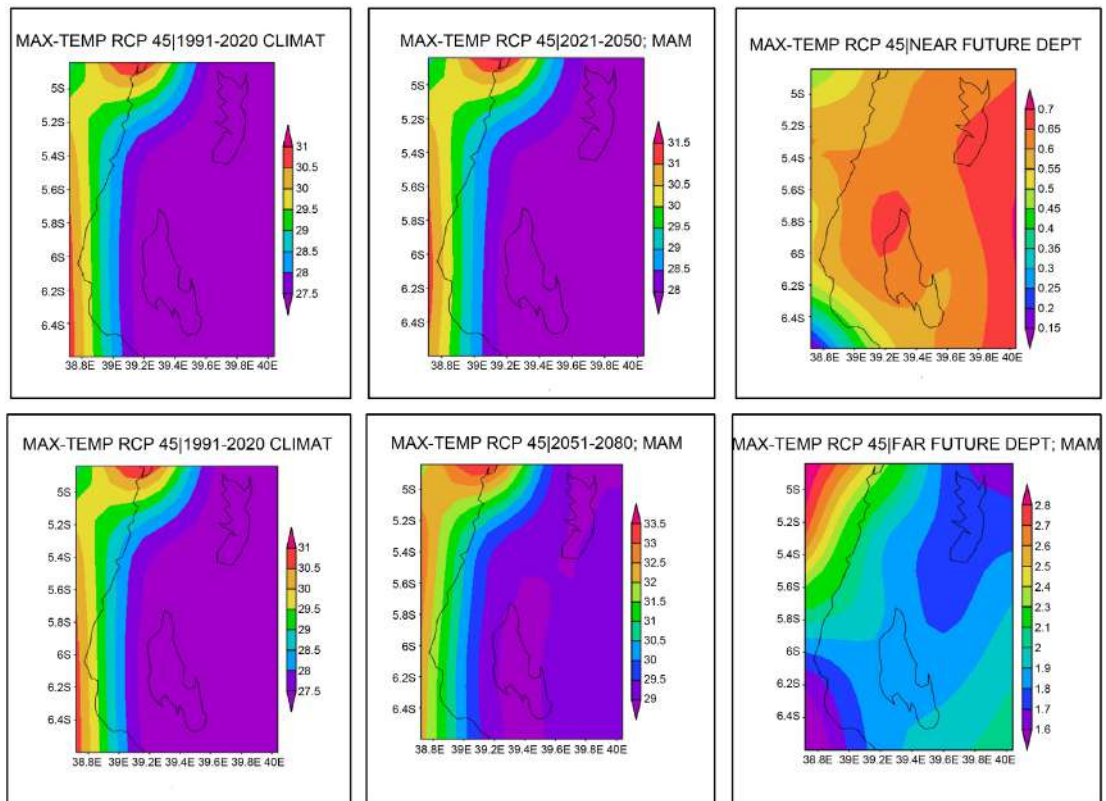


Figure 13. Maximum temperature ($^{\circ}$ C) in MAM seasonal variation under RCP 4.5.

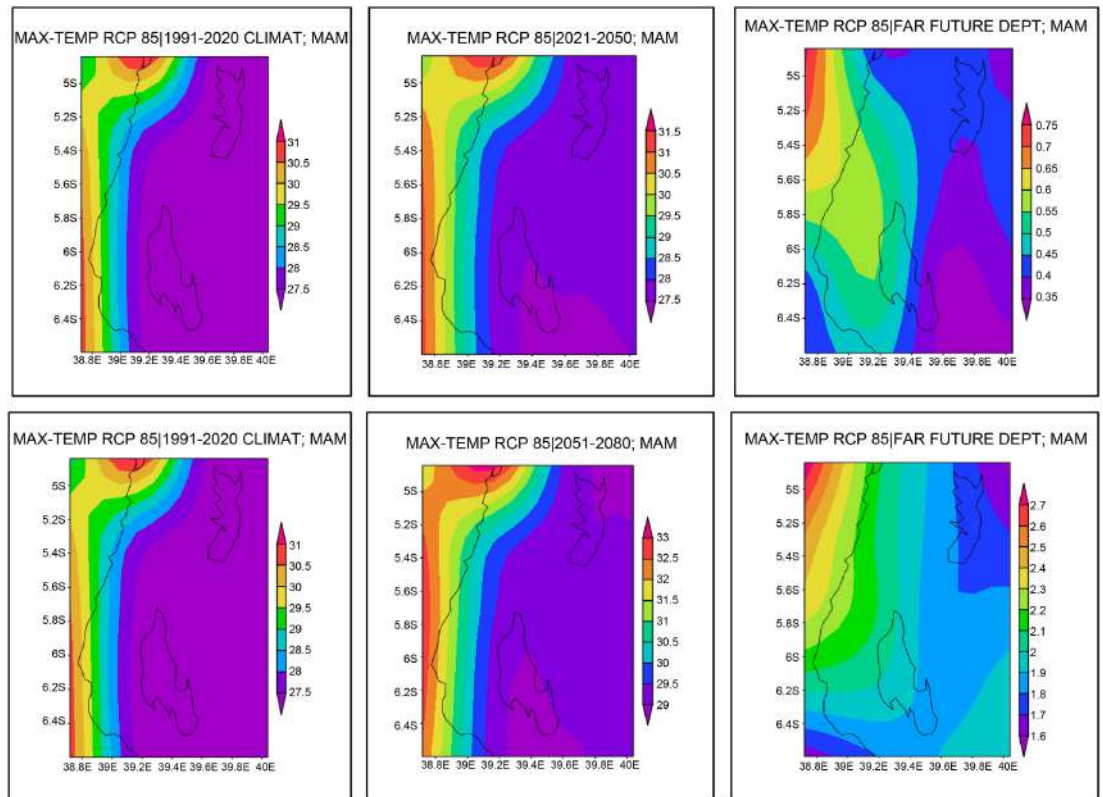


Figure 14. Maximum temperature ($^{\circ}$ C) in MAM seasonal variation under RCP 8.5.

ranging from 1.7°C - 1.8°C to 1.7°C - 2.0°C compared to 0.4°C - 0.45°C to 0.6°C - 0.7°C NF respectively. As for the OND, the projected mean T_{max} under RCP 4.5 and RCP 8.5 presented in **Figure 15** and **Figure 16** upper left and middle; lower left panel) show that mean T_{max} during OND is projected to increase from the range of 25.2°C to 25.5°C - 26°C (HS) to 26°C - 27.5°C - 28.0°C (NF); 27°C - 27.5°C (FF) for both Unguja and Pemba (**Figure 15** and **Figure 16** upper left and middle panel) and in (**Table 3**). T_{max} in FF were higher ranged 1.5°C to 2.0°C in both RCPs compared to 0.6°C - 0.9°C for RCP 4.5 and 0.3 - 0.6 under RCP 8.5 scenario of NF. The results are concurred with [48] that the maximum temperature departure in Zanzibar is projected to increase from 0.5°C - 1.4°C for RCP 4.5 and from 0.6°C - 2.8°C RCP 8.5 (NF-FF) respectively.

3.9. The Projections of March to May and October-December Minimum Temperature Variation under RCP 4.5 and RCP 8.5

The results of the projected mean T_{min} under RCP 4.5 and RCP 8.5 presented in **Figure 17** and **Figure 18** show that the mean T_{min} during MAM is projected to increase with time from the range of 25.5 (HS) to 26.0°C - 27.0°C (NF); 27.5 (FF) for both Unguja and Pemba (**Figure 17** and **Figure 20** upper left and middle;

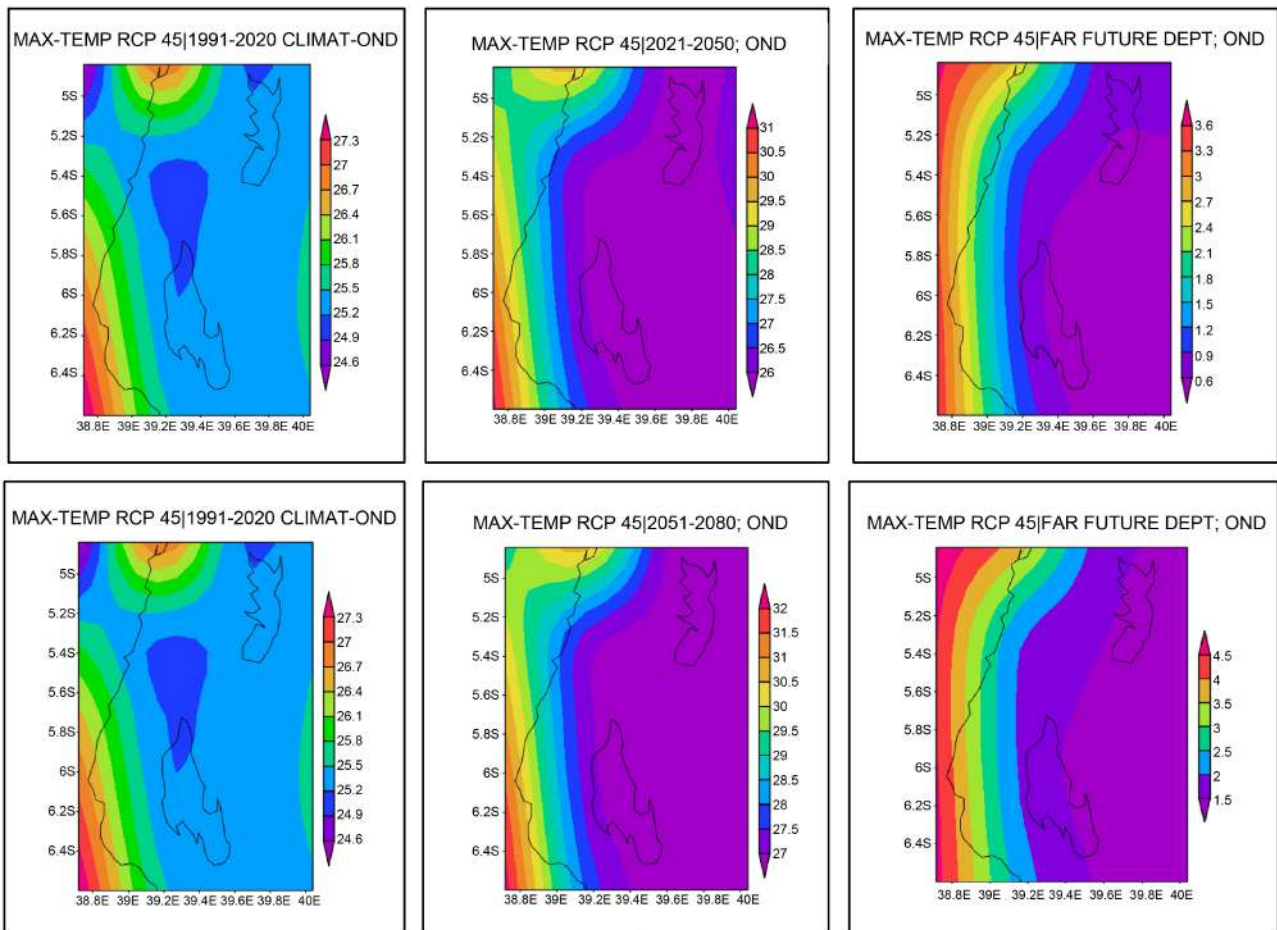


Figure 15. Maximum temperature (°C) in OND seasonal variation under RCP 4.5.

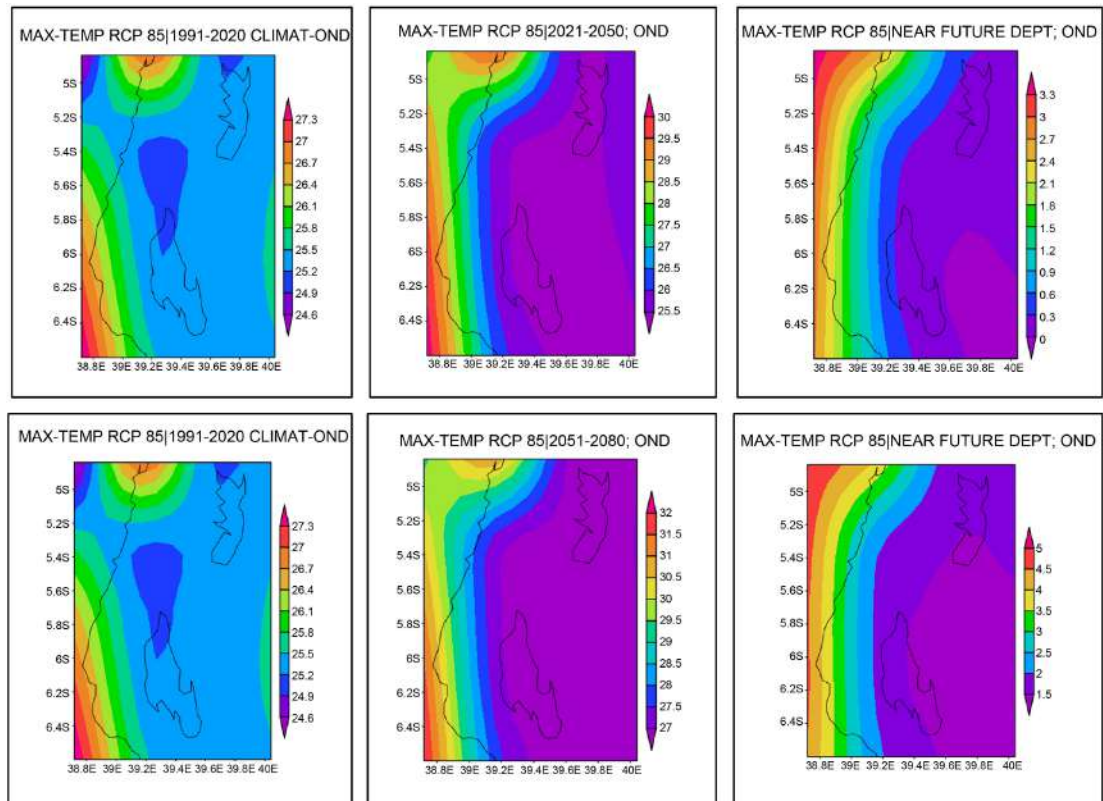


Figure 16. Maximum temperature ($^{\circ}\text{C}$) in OND seasonal variation under RCP 8.5.

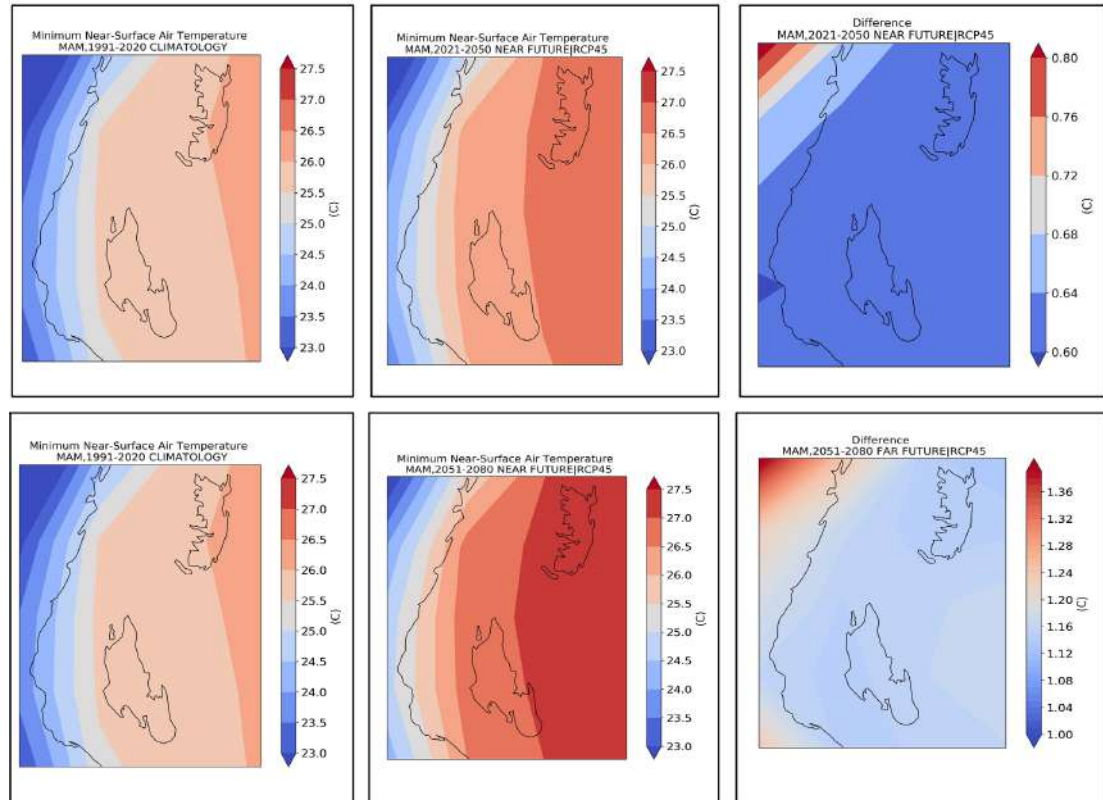


Figure 17. Minimum temperature in MAM seasonal variation under RCP 4.5.

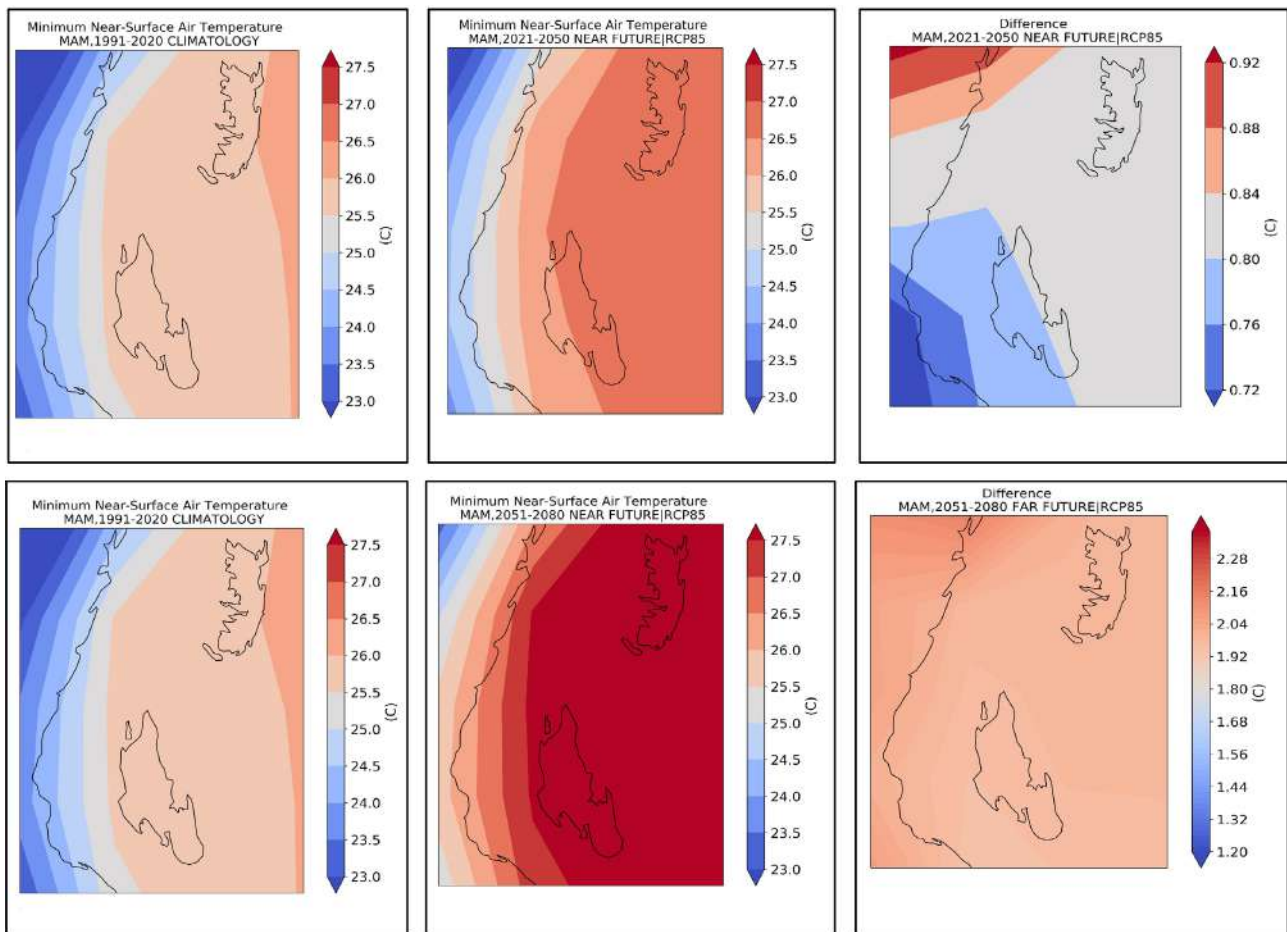


Figure 18. Minimum temperature in MAM seasonal variation under RCP 8.5.

Table 3. The summarized results of maximum temperature projection on MAM and OND season under RCP 4.5 and RCP8.5 in both Unguja and Pemba islands.

Parameter:	RCP 4.5				RCP 8.5			
	MAM season		OND season		MAM season		OND season	
	NF	FF	NF	FF	NF	FF	NF	FF
UNGUJA	Increasing from 0.5 - 0.6	Increasing from 1.8 - 1.9	Increasing from 0.6 - 0.9	Increasing from 1.5 - 2.0	Increasing from 0.35 - 0.4	Increasing from 1.8 - 2.0	Increasing from 0.3 - 0.6	Increasing from 1.5 - 2.0
PEMBA	Increasing from 0.6 - 0.7	Increasing from 1.7 - 1.8	Increasing from 0.6 - 0.9	Increasing from 1.5 - 2.0	Increasing from 0.4 - 0.45	Increasing from 1.7 - 1.8	Increasing from 0 - 0.3	Increasing from 1.5 - 2.0

lower left panel). FF in the MAM season depicted higher T_{min} under RCP 4.5 and RCP 8.5 ranging from 1.12°C - 1.16°C to 1.92°C - 2.04°C compared to 0.6°C - 0.64°C to 0.76°C - 0.84°C NF, respectively (upper and lower right panel). As for the OND, the projected mean T_{min} under RCP 4.5 and RCP 8.5 presented in **Figure 19** and **Figure 20** show that the mean T_{min} during OND is projected to increase from the range of 25.5°C - 26.0°C (HS) to 26°C - 26.5°C (NF); 27°C -

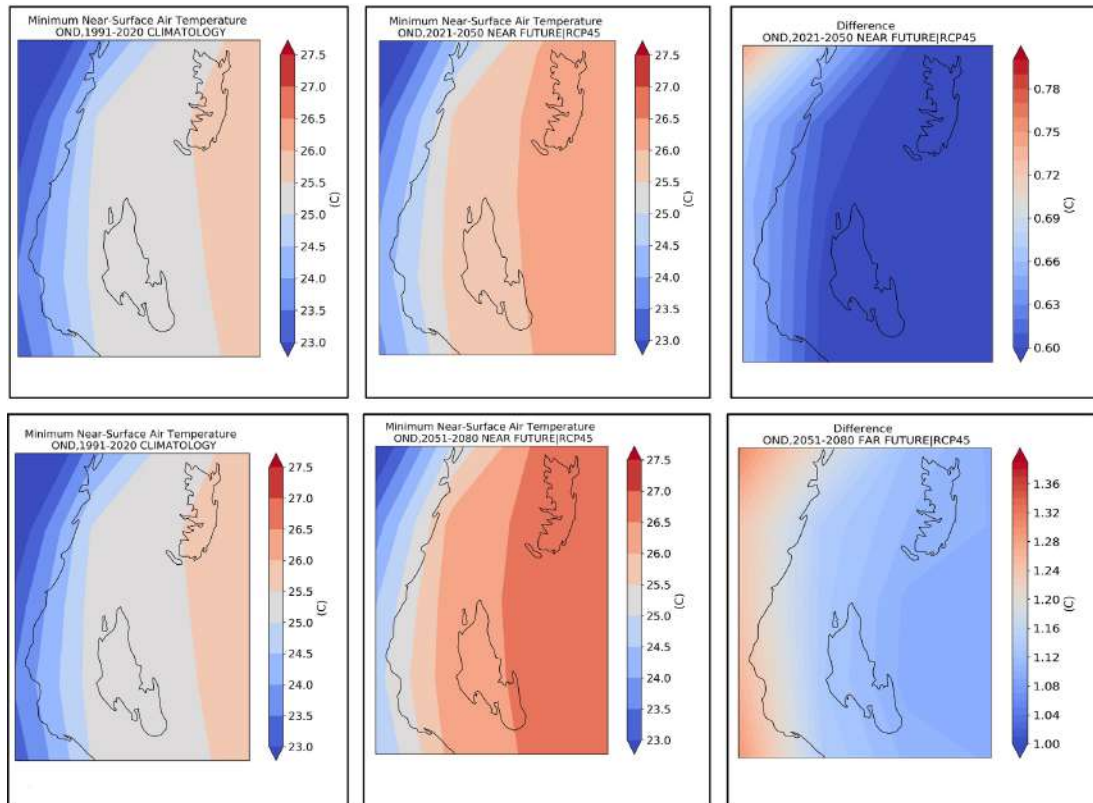


Figure 19. Minimum temperature in OND seasonal variation under RCP 4.5.

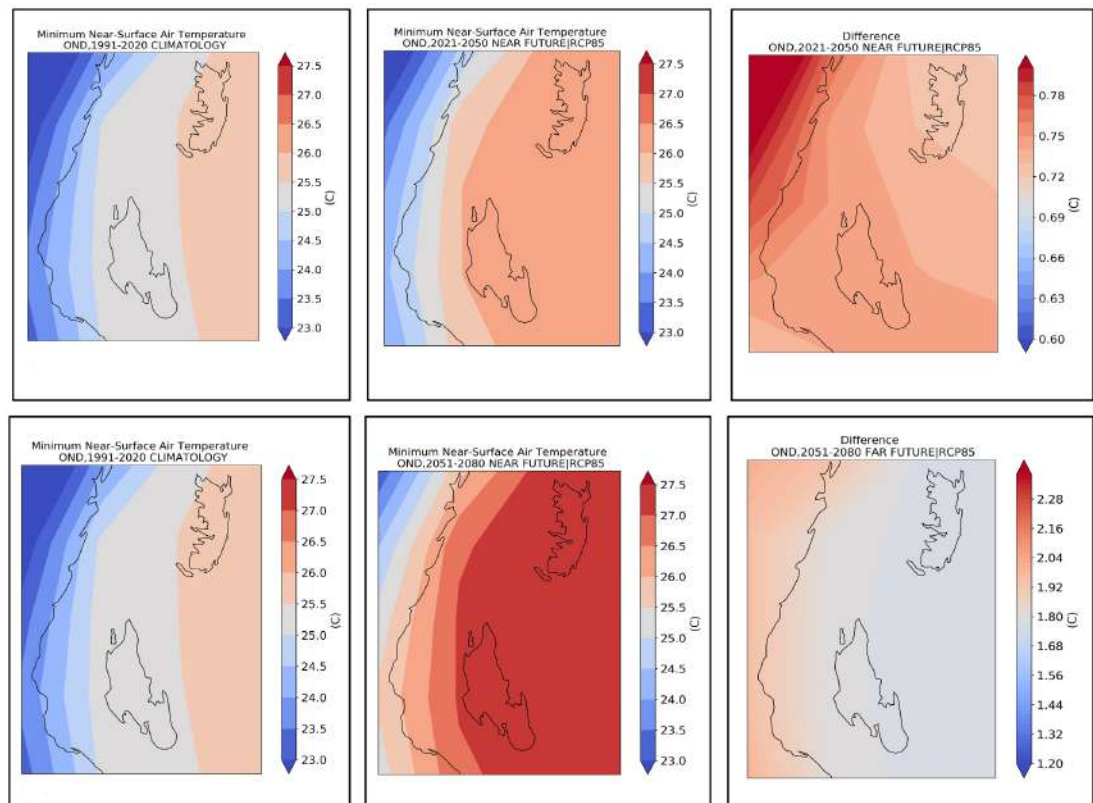


Figure 20. Minimum temperature in OND seasonal variation under RCP 8.5.

27.5°C (FF) for both Unguja and Pemba (Figure 19 and Figure 20 upper left and middle; lower left panel) and in (Table 4), T_{\min} in FF under RCP 4.5 and RCP 8.5 were higher ranged 1.12°C - 1.16°C to 1.8°C to 1.92°C compared to 0.6°C - 0.63°C for RCP 4.5 and 0.6°C - 0.75°C under RCP 8.5 scenario of NF, (upper and lower right panel). These results concurred with IPCC indicating a global average warming of 0.85°C over the period 1880 to 2012 with increasing of the number of warm days and nights on a global scale [2] [47] [48].

4. Discussion

Climate change is a global phenomenon, with varying intensities and impacts from one region to another. These climate change impacts have resulted in serious social-economic ramifications associated with the increased frequency of extreme weather events worldwide including Tanzania and Zanzibar in particular. Serious floods and ever-recorded higher temperatures have been observed and reported in recent years. The study was aimed at understanding the extent to which variability of spatial-temporal trends was affected, also the study investigated the future trends of these climate variables for the near future (NF) and far future (FF) regarding the historical records (HS) under two RCPs of 4.5 and 8.5, respectively. Besides, the extremely wet and dry periods were investigated using the SPI to show the impact of climate change on the rainfall patterns of Zanzibar.

The presented SPI results in Figure 2(a) show the existence of climate shift (*i.e.* SPI values changed from near normal to moderate wet reaching to extremely wet during the last decades at Zanzibar Airport and Matangatuani in Pemba) indicating that climate change has influenced rainfall resulting in higher wetter conditions due to strengthened seasonal rainfall. Also, the presented results have shown that some areas including Mahonda have been affected by dryness conditions due to weaken seasonally (Figure 2(b)). Generally, the presented incidence indicates that the existing climate change impacts on rainfall distribution in Pemba have resulted in declining/enhancing rainfall in most areas in Zanzibar, especially over the last ten years. The study SPI within the island concurred with [21] who detected severe drought during both long and short growing seasons events in Pemba in 1975, 1991, 2003 and 2004. Moreover, our study results are agreed with [20] who noted the significant socioeconomic ramifications (ranging from floods to loss of life) due to increased rainfall strengths during OND 2019, MAM 2020 and the 2020 January to February (*i.e.* the off-season rainfall January to February 2020) which led to negative impacts on agriculture.

Further results for understanding the rainfall trends in Zanzibar are the observed Mann–Kendall monotonic trends which have shown the highest p values and most rapid positive increase of slope in the urban west region of Unguja as compared to northern and southern regions, indicating higher rainfall in the urban west and its rural areas than the rest part of Unguja, and for Pemba p values was higher to northern compared to southern regions, the rainfall distribution in amount is slightly at Pemba Airport and near regions. Higher rainfall at

Table 4. The summarized results of minimum temperature projection on MAM and OND seasons under RCP 4.5 and RCP8.5 in both Unguja and Pemba islands.

Parameter: Min Temp (°C)	RCP 4.5				RCP 8.5			
	MAM season		OND season		MAM season		OND season	
	NF	FF	NF	FF	NF	FF	NF	FF
UNGUJA	Increasing from 0.6 - 0.64	increasing from 1.12 - 1.16	increasing from 0.6 - 0.63	increasing from 1.12 - 1.16	increasing from 0.76 - 0.8	increasing from 1.92 - 2.04	increasing from 0.72 - 0.75	Increasing from 1.8 - 1.92
PEMBA	Increasing from 0.6 - 0.64	Increasing from 1.12 - 1.16	Increasing from 0.6 - 0.63	Increasing from 1.12 - 1.16	increasing from 0.8 - 0.84	increasing from 1.92 - 2.04	Increasing from 0.60 - 0.72	Increasing from 1.8 - 1.92

Mkoani followed by Wete which indicates that Mkoani is leading compared to other regions. The impacts of the observed higher rainfall over most areas of Zanzibar is in concurrence with [24] who noted that higher rainfall in OND 2019 has resulted into a number of socioeconomic stresses including the death of people, damage to electric poles resulting in power shortage for several days (at Mwakaje and Mwera) also trees and vegetation plantation were affected.

The presented results on the influence of climate change on spatial rainfall distribution for the three-time period of D1, D2 and D3 revealed shifts of rainfall intensities associated with an increasing trend during the MAM season with high intensities (1423 - 1572 mm) in Pemba Island compare to Unguja (994 - 1022 mm). As for the short rain period of OND the presented results have shown a significant increase in Pemba island during D3. More results have shown that the annual rainfall was characterized by increasing rates from D1 to D2 and a slight decrease during D3 over the northern parts of Unguja island, with higher intensities in Kizimbani, Zanzibar airport and part of central parts of Unguja and (Chake - Chake district in Pemba. The presented results on higher intensity with good spatial and temporal rainfall distribution during D3 are well agreed with [20] [24] who noted that the increased frequency of severe weather events (extreme rainfall due to the existence of extreme climate and oceanographic factors associated with climate change) induced extreme wetness of three consecutive seasons of MAM, 2019, OND, 2019 and JF (2020) of seasonal rainfall in Tanzania and the northern coastal area in particular.

As for the climate influence on T_{max} and T_{min} at Unguja and Pemba, the presented results have shown that T_{max} was increasing at the rate of 0.035 and 0.0169°C/yr, respectively. Similar results hold for T_{min} indicating a warming trend of 0.064°C/yr and 0.104°C/yr indicating increasing day-to-night warmer conditions results as compared to the past. These study results are in agreement with worldwide observed higher temperature trends as documented by [2] [3] [49] as well as [47] that on a global scale, the global average warming has increased by 0.85°C from 1880 to 2012 with an increasing number of warm days and nights.

The presented projection results for the NF, and FF with respect to historical (HS) have shown that MAM rainfall projection under RCP 4.5 in Unguja and Pemba island are in decreasing and increasing modes spatially in NF and FF respectively. Also, results have shown that under RCP 8.5, Unguja and Pemba are characterized by decreasing/increasing rainfall (by a range of 25 mm) in the NF, and vice versa for the FF. As for the OND rainfall, the presented projection results under RCP 4.5 and RCP 8.5 revealed a decreasing rainfall in Unguja at a range of 25 - 50 mm and 0 - 25 for both NF and FF, while Pemba is characterized by an increasing rainfall of 0 - 25 mm for FF under both RCPs, while increasing/decreasing at the same under RCP 8.5/4.5 in NF (**Table 4**). The study results are in agreement/disagreement with [48] for Pemba and Unguja under both RCPs and both time periods (NF and FF).

The presented projection results for the MAM and OND T_{max} under RCP 4.5 and 8.5 in Unguja and Pemba depicted an increasing T_{max} with time. For instance, FF has depicted higher T_{max} ranging from $1.7^{\circ}\text{C} - 1.8^{\circ}\text{C}$ to $1.7^{\circ}\text{C} - 2.0^{\circ}\text{C}$ under RCP 4.5 and 8.5 compared to NF during MAM. As for the OND seasons, T_{max} during FF was higher ranged 1.5°C to 2.0°C in both RCPs compared to $0.6^{\circ}\text{C} - 0.9^{\circ}\text{C}$ for RCP 4.5 and $0.3 - 0.6$ under the RCP 8.5 scenario of NF. More presented projection results for T_{min} revealed an increasing trend under both time slices (NF and FF) and under both RCPs (4.5 and 8.5). For instance, Under RCP 4.5 during MAM and OND season, the projected T_{min} were increasing in a range of 0.6°C to 0.64°C during NF and $1.12^{\circ}\text{C} - 1.16^{\circ}\text{C}$ during FF, while for the RCP 8.5, the projected T_{min} was 0.76°C to 0.84°C in NF and 1.12°C to 1.16°C FF in MAM, and from $0.69^{\circ}\text{C} - 0.72^{\circ}\text{C}$ to $1.8^{\circ}\text{C} - 1.92^{\circ}\text{C}$ during OND. These projected results of increasing max and T_{min} indicate that the current climate is expected to experience warmer conditions resulting to an increasing number of hot days and warm nights compared to the past. The study results are in agreement with [2] [6] [47] who noted an increased number of warm days and nights on global regional and local scales. The presented study findings suggest the formulation of effective adaptation strategies to adapt to the projected increase in T_{max} and T_{min} as well as the increased rates of severe weather events in Zanzibar.

5. Conclusions

This study presented the three decades of 1991-2000 (hereafter D1), 2001-2010 (hereafter D2) and 2011-2020 (hereafter D3) to analyze periodical spatial rainfall distribution in Zanzibar as well as projection for Zanzibar (Unguja and Pemba islands) based on climate simulations from high resolution CORDEX regional climate models. We have found that:

- 1) There is an existence of climate shift in 2005 from lower to higher temperature with changes ranging from 0.7% - 1.6% for T_{max} and 2.72% - 7.1% for T_{min} in Unguja and Pemba, indicating increased warming resulting in a higher number of hot days and warm nights which affects the socio-economics of the

peoples in Zanzibar.

2) The severe weather events result in extreme wet and dry conditions in Zanzibar for instance Zanzibar Airport and Matangatuani in Pemba had shown moderate wet conditions, while the northern part of Unguja (Mahonda) and Pemba airport have shown normal to moderately dry conditions.

3) Long-term rainfall trends are showing increased rainfall intensities in Urban west in Unguja, whereas Mkoani in Pemba had shown higher rainfall trends compared to other regions.

4) The second decade of the 21st century (D3) has shown higher MAM and OND rainfall intensities in most areas of Unguja and Pemba including the Urban West region (Unguja) compared to other regions and periods.

5) Projected rainfall is likely to decrease in Unguja in the range of 25 - 50 mm while increasing in a range of 0 - 25 mm in Pemba for NF and FF and for both RCPs.

6) Projected T_{\max} in Zanzibar (Unguja and Pemba) is likely to increase in FF in the range of 1.7°C - 2.0°C compared to 0.3°C - 0.9°C NF for both RCPs.

7) Projected T_{\min} in Zanzibar is likely to increase in FF with higher values ranging from 1.12°C to 1.16°C compared to 0.69°C - 0.72°C in NF for both RCPs.

Recommendation

Based on the presented discussion and conclusions, the study recommends for more studies be conducted to gain a clear understanding of the impacts of climate change in different time scales and different areas of Zanzibar. Secondly, the formulation of effective adaptation, strategies and resilience mechanisms to combat the projected climate change impacts especially in the agricultural sector, water and food security. Lastly, calls for the restructuring of urban planning, to cope with the influence of the undergoing impacts of climate change.

Acknowledgements

The authors are grateful to the Tanzania Meteorological Authority for the provision of observed meteorological data used and to CORDEX Africa for providing model data used in this study. Thanks to all individuals to whom in all steps of organizing this paper and TMA staffs administration are highly acknowledged for financial support to awards finalizing the materials for this paper and granting the permission for the first author to go for his master's degree.

Conflicts of Interest

The authors declare no conflicts of interest regarding the publication of this paper.

References

- [1] IPCC (2007) Climate Change 2007: The Physical Science Basis. Contribution of

- Working Group I to the Fourth Assessment Report of the Intergovernmental Panel on Climate Change. Cambridge University Press, Cambridge, 996.
- [2] IPCC Panel (2014) Climate Change 2014: Synthesis Report. 1-151.
 - [3] Intergovernmental Panel on Climate Change (IPCC) (2013) Climate Change 2013: The Physical Science Basis. Working Group I Contribution to the Fifth Assessment Report of the Intergovernmental Panel on Climate Change. Cambridge University Press, Cambridge. <https://doi.org/10.1017/CBO9781107415324>
 - [4] Collins, J.M. (2011) Temperature Variability over Africa. *Journal of Climate*, **24**, 3649-3666. <https://doi.org/10.1175/2011JCLI3753.1>
 - [5] Sutton, R.T., Dong, B. and Gregory, J.M. (2007) Land/Sea Warming Ratio in Response to Climate Change: IPCC AR4 Model Results and Comparison with Observations. *Geophysical Research Letters*, **34**, L02701. <https://doi.org/10.1029/2006GL028164>
 - [6] Osima, S., Indasi, V.S., Zaroug, M., Endris, H.S., Gudoshava, M., Misiani, H.O., Nimusiima, A., Anyah, R.O., Otieno, G., Ogwang, B.A. and Jain, S. (2018) Projected Climate over the Greater Horn of Africa under 1.5 °C and 2 °C Global Warming. *Environmental Research Letters*, **13**, Article ID: 065004. <https://doi.org/10.1088/1748-9326/aabab>
 - [7] Ahmed, S.A., Diffenbaugh, N.S. and Hertel, T.W. (2009) Climate Volatility Deepens Poverty Vulnerability in Developing Countries. *Environmental Research Letters*, **4**, Article ID: 034004. <https://doi.org/10.1088/1748-9326/4/3/034004>
 - [8] Hansen, J., Ruedy, R., Sato, M. and Lo, K. (2010) Global Surface Temperature Change. *Reviews of Geophysics*, **48**, RG4004. <https://doi.org/10.1029/2010RG000345>
 - [9] Ouarda, T.B., Charron, C., Kumar, K.N., Marpu, P.R., Ghedira, H., Molini, A. and Khayal, I. (2014) Evolution of the Rainfall Regime in the United Arab Emirates. *Journal of Hydrology*, **514**, 258-270. <https://doi.org/10.1016/j.jhydrol.2014.04.032>
 - [10] Baigorria, G.A. and Jones, J.W. (2010) GiST: A Stochastic Model for Generating Spatially and Temporally Correlated Daily Rainfall Data. *Journal of Climate*, **23**, 5990-6008. <https://doi.org/10.1175/2010JCLI3537.1>
 - [11] Raziei, T., Daryabari, J., Bordi, I. and Pereira, L.S. (2014) Spatial Patterns and Temporal Trends of Precipitation in Iran. *Theoretical and Applied Climatology*, **115**, 531-540. <https://doi.org/10.1007/s00704-013-0919-8>
 - [12] Nam, W. and Baigorria, G.A. (2015) How Climate Change Has Affected the Spatio-Temporal Patterns of Precipitation and Temperature at Various Time Scales in North Korea. *International Journal of Climatology*, **36**, 722-734. <https://doi.org/10.1002/joc.4378>
 - [13] Field, C.B. and Barros, V.R. (2014) Climate Change 2014-Impacts, Adaptation and Vulnerability: Regional Aspects. Cambridge University Press, Cambridge.
 - [14] Tierney, J.E., Ummenhofer, C.C. and Demenocal, P.B. (2015) Past and Future Rainfall in the Horn of Africa. *Science Advances*, **1**, e1500682. <https://doi.org/10.1126/sciadv.1500682>
 - [15] Gebrechorkos, S.H., Hülsmann, S. and Bernhofer, C. (2019) Long-Term Trends in Rainfall and Temperature Using High-Resolution Climate Datasets in East Africa. *Scientific Reports*, **9**, Article No. 11376. <https://doi.org/10.1038/s41598-019-47933-8>
 - [16] Endris, H.S., Lennard, C., Hewitson, B., Dosio, A., Nikulin, G. and Panitz, H.J. (2016) Teleconnection Responses in Multi-GCM Driven CORDEX RCMs over Eastern Africa. *Climate Dynamics*, **46**, 2821-2846. <https://doi.org/10.1007/s00382-015-2734-7>

- [17] Fer, I., Tietjen, B., Jeltsch, F. and Wolff, C. (2017) The Influence of El Niño-Southern Oscillation Regimes on Eastern African Vegetation and Its Future Implications under the RCP8.5 Warming Scenario. *Biogeosciences*, **14**, 4355-4374. <https://doi.org/10.5194/bg-14-4355-2017>
- [18] Mpelasoka, F., Awange, J.L. and Zerihun, A. (2018) Influence of Coupled Ocean-Atmosphere Phenomena on the Greater Horn of Africa Droughts and Their Implications. *Science of the Total Environment*, **610**, 691-702. <https://doi.org/10.1016/j.scitotenv.2017.08.109>
- [19] Endris, H.S., Omondi, P., Jain, S., Lennard, C., Hewitson, B., Chang'a, L., Awange, J.L., Dosio, A., Ketiemi, P., Nikulin, G. and Panitz, H.J. (2013) Assessment of the Performance of CORDEX Regional Climate Models in Simulating East African Rainfall. *Journal of Climate*, **26**, 8453-8475. <https://doi.org/10.1175/JCLI-D-12-00708.1>
- [20] Kai, K.H., Kijazi, A.L. and Osima, S.E. (2020) An Assessment of the Seasonal Rainfall and 16 Its Societal Implications in Zanzibar Islands during the Season of October to December, 2019. *Atmospheric and Climate Sciences*, **10**, 509-529. <https://doi.org/10.4236/acs.2020.104026>
- [21] Hassan, I.H., Mdemu, M.V., Shemdoe, R.S. and Stordal, F. (2014) Drought Pattern along the Coastal Forest Zone of Tanzania. *Atmospheric and Climate Sciences*, **4**, 369-384. <https://doi.org/10.4236/acs.2014.43037>
- [22] Mtongori, H.I., Stordal, F. and Benestad, R.E. (2016) Evaluation of Empirical Statistical Downscaling Models' Skill in Predicting Tanzanian Rainfall and Their Application in Providing Future Downscaled Scenarios. *Journal of Climate*, **29**, 3231-3252. <https://doi.org/10.1175/JCLI-D-15-0061.1>
- [23] Chikodzi, D., Murwendo, T. and Simba, F.M. (2013) Climate Change and Variability in Southeast Zimbabwe: Scenarios and Societal Opportunities. *American Journal of Climate Change*, **2**, 36-46. <https://doi.org/10.4236/ajcc.2013.23A004>
- [24] Kai, K.H., Osima, S.E., Kijazi, A.L., Ngwali, M.K. and Hamad, A.O. (2021) Assessment of the Off-Season Rainfall of January to February 2020 and Its Socio Economic Implications in Tanzania: A Case Study of the Northern Coast of Tanzania. *Journal of Atmospheric Science Research*, **4**, 51-69. <https://doi.org/10.30564/jasr.v4i2.3135>
- [25] OCGS (Office of the Chief Government Statistician) (2022) Zanzibar in Figures, 2022.
- [26] Kijazi, A.L. and Reason, C.J.C. (2005) Relationships between Intraseasonal Rainfall Variability of Coastal Tanzania and ENSO. *Theoretical and Applied Climatology*, **82**, 153-176. <https://doi.org/10.1007/s00704-005-0129-0>
- [27] Mahongo, S.B., Francis, J. and Osima, S.E. (2011) Wind Patterns of Coastal Tanzania: Their Variability and Trends. *Western Indian Ocean Journal of Marine Science*, **10**, 107-120.
- [28] Watkiss, P., Pye, S., Hendriksen, G., Maclean, A., Bonjean, M., Jiddawi, N., Shaghude, Y. and Sheikh, M.A. (2012) The Economics of Climate Change in Zanzibar. 1-36.
- [29] McKee, T.B., Doesken, N.J. and Kleist, J. (1993) The Relationship of Drought Frequency and Duration to Time Scales. In: *Proceedings of the 8th Conference on Applied Climatology*, American Meteorological Society, Boston, 179-184.
- [30] WMO (2012) Standardized Precipitation Index User Guide 1090. https://www.droughtmanagement.info/literature/WMO_standardized_precipitation_index_user_guide_en_2012.pdf

- [31] Lukali, A.A., Osima, S.E., Lou, Y. and Kai, K.H. (2021) Assessing the Impacts of Climate Change and Variability on Maize (*Zea mays*) Yield over Tanzania. *Atmospheric and Climate Sciences*, **11**, 569-588. <https://doi.org/10.4236/acs.2021.113035>
- [32] Agbo, E.P., Ekpo, C.M. and Edet, C.O. (2021) Analysis of the Effects of Meteorological Parameters on Radio Refractivity, Equivalent Potential Temperature and Field Strength via Mann-Kendall Test. *Theoretical and Applied Climatology*, **143**, 1437-1456. <https://doi.org/10.1007/s00704-020-03464-1>
- [33] Hayelom, B., Chen, Y., Marsie, Z. and Negash, M. (2017) Temperature and Precipitation Trend Analysis over the Last 30 Years in Southern Tigray Regional State, Ethiopia. <https://doi.org/10.20944/preprints201702.0014.v1>
- [34] Wu, Y., Wang, W. and Wang, G. (2016) Detecting Variation Trends of Temperature and Precipitation for the Dadu River Basin, China. *Advances in Meteorology*, **2016**, Article ID: 2564586. <https://doi.org/10.1155/2016/2564586>
- [35] Arora, M., Goel, N.K. and Singh, P. (2005) Evaluation of Temperature Trends over India/Evaluation de tendances de température en Inde. *Hydrological Sciences Journal*, **50**, 93. <https://doi.org/10.1623/hysj.50.1.81.56330>
- [36] Fan, X.H. and Wang, M.B. (2011) Change Trends of Air Temperature and Precipitation over Shanxi Province, China. *Theoretical and Applied Climatology*, **103**, 519-531. <https://doi.org/10.1007/s00704-010-0319-2>
- [37] Kisi, O. and Ay, M. (2014) Comparison of Mann-Kendall and Innovative Trend Method for Water Quality Parameters of the Kizilirmak River, Turkey. *Journal of Hydrology*, **513**, 362-375. <https://doi.org/10.1016/j.jhydrol.2014.03.005>
- [38] Pal, A.B., Khare, D., Mishra, P.K. and Singh, L. (2017) Trend Analysis of Rainfall, Temperature and Runoff Data: A Case Study of Rangoon Watershed in Nepal. *International Journal of Students' Research in Technology & Management*, **5**, 21-38. <https://doi.org/10.18510/ijstrtm.2017.535>
- [39] Dawood, M., Mahmood, S., Rahman, G. and Rahman, A.U. (2017) Impact of Rainfall Fluctuation on River Discharge in Hindu Kush Region, Pakistan. *Abasyn Journal of Social Sciences*, **10**, 246-259.
- [40] Mandale, V.P., Mahale, D.M., Nandgude, S.B., Gharde, K.D. and Thokal, R.T. (2017) Spatio-Temporal Rainfall Trends in Konkan Region of Maharashtra State. *Advanced Agricultural Research & Technology Journal*, **1**, 61-69.
- [41] Mandale, V.P., Mahale, D.M., Nandgude, S.B., Gharde, K.D. and Thokal, R.T. (2017) Spatio-Temporal Rainfall Trends in Konkan Region of Maharashtra State. *Advanced Agricultural Research & Technology Journal*, **1**, 61-69.
- [42] Sen, P.K. (1968) Estimates of the Regression Coefficient Based on Kendall's Tau. *Journal of the American Statistical Association*, **63**, 1379-1389. <https://doi.org/10.1080/01621459.1968.10480934>
- [43] Longley, P.A., Goodchild, M.F., Maguire, D.J. and Rhind, D.W. (2001) New Developments in Geographical Information Systems; Principles, Techniques, Management and Applications. In: Longley, P., Ed., *Geographical Information Systems: Principles, Techniques, Management and Applications*, 2nd Edition, John Wiley & Sons Inc., Hoboken, 404.
- [44] Debnath, P. (2022) A QGIS-Based Road Network Analysis for Sustainable Road Network Infrastructure: An Application to the Cachar District in Assam, India. *Infrastructures*, **7**, 114. <https://doi.org/10.3390/infrastructures7090114>
- [45] Setianto, A. and Triandini, T. (2013) Comparison of Kriging and Inverse Distance Weighted (IDW) Interpolation Methods in Lineament Extraction and Analysis. *Journal of Applied Geology*, **5**. <https://doi.org/10.22146/jag.7204>

- [46] Paramasivam, C.R. and Venkatramanan, S. (2019) An Introduction to Various Spatial Analysis Techniques. In: Venkatramanan, S., Prasanna, M.V. and Chung, S.Y., Eds., *GIS and Geostatistical Techniques for Groundwater Science*, Elsevier, Amsterdam, 23-30. <https://doi.org/10.1016/B978-0-12-815413-7.00003-1>
- [47] Chang'a, L.B., Kijazi, A.L., Luhunga, P.M., Ng'ongolo, H.K. and Mtongori, H.I. (2017) Spatial and Temporal Analysis of Rainfall and Temperature Extreme Indices in Tanzania. *Atmospheric and Climate Sciences*, **7**, 525-539. <https://doi.org/10.4236/acs.2017.74038>
- [48] Luhunga, P.M., Kijazi, A.L., Chang'a, L., Kondowe, A., Ng'ongolo, H. and Mtongori, H. (2018) Climate Change Projections for Tanzania Based on High-Resolution Regional Climate Models from the Coordinated Regional Climate Downscaling Experiment (CORDEX)-Africa. *Frontiers in Environmental Science*, **6**, 122. <https://doi.org/10.3389/fenvs.2018.00122>
- [49] IPCC (2012) Managing the Risks of Extreme Events and Disasters to Advance Climate Change Adaptation. In: Field, C.B., Barros, V., Stocker, T.F., *et al.*, Eds., *A Special Report of Working Groups I and II of the Intergovernmental Panel on Climate Change*, Cambridge University Press, Cambridge.